Epigenetic Control of Learning and Memory in *Drosophila* by Tip60 HAT Action

Songjun Xu, Rona Wilf, Trisha Menon, Priyalakshmi Panikker, Jessica Sarthi, and Felice Elefant[1]
Department of Biology, Drexel University, Philadelphia, Pennsylvania 19104

ABSTRACT Disruption of epigenetic gene control mechanisms in the brain causes significant cognitive impairment that is a debilitating hallmark of most neurodegenerative disorders, including Alzheimer's disease (AD). Histone acetylation is one of the best characterized of these epigenetic mechanisms that is critical for regulating learning- and memory- associated gene expression profiles, yet the specific histone acetyltransferases (HATs) that mediate these effects have yet to be fully characterized. Here, we investigate an epigenetic role for the HAT Tip60 in learning and memory formation using the *Drosophila* CNS mushroom body (MB) as a well-characterized cognition model. We show that Tip60 is endogenously expressed in the Kenyon cells, the intrinsic neurons of the MB, and in the MB axonal lobes. Targeted loss of Tip60 HAT activity in the MB causes thinner and shorter axonal lobes while increasing Tip60 HAT levels cause no morphological defects. Functional consequences of both loss and gain of Tip60 HAT levels in the MB are evidenced by defects in immediate-recall memory. Our ChIP-Seq analysis reveals that Tip60 target genes are enriched for functions in cognitive processes, and, accordingly, key genes representing these pathways are misregulated in the Tip60 HAT mutant fly brain. Remarkably, we find that both learning and immediate-recall memory deficits that occur under AD-associated, amyloid precursor protein (APP)-induced neurodegenerative conditions can be effectively rescued by increasing Tip60 HAT levels specifically in the MB. Together, our findings uncover an epigenetic transcriptional regulatory role for Tip60 in cognitive function and highlight the potential of HAT activators as a therapeutic option for neurodegenerative disorders.

THE ability of living organisms to respond to a constantly changing environment and fine-tune their complex behaviors accordingly is crucial for their adaptation and survival throughout development (Levenson and Sweatt 2005; Borrelli *et al.* 2008; West and Greenberg 2011; Al-Saigh *et al.* 2012). One of the most important of such experience-driven behavioral changes is learning and memory formation, as it directly impacts cognitive ability (Levenson and Sweatt 2005; Carulli *et al.* 2011; Nelson and Monteggia 2011; West and Greenberg 2011). In the brain, external stimuli are converted into intracellular signals that program coordinated expression of specific gene sets that promote sustained neuroplasticity and cognitive adaptation (Sweatt 2009; Riccio 2010; Carulli *et al.* 2011). Disruption of these response programs results in significant cognitive impairment disorders (West and Greenberg 2011; Ebert and Greenberg 2013; Pirooznia and Elefant 2013a). Epigenetic post-translational modifications (PTMs) of histone proteins that control nuclear chromatin packaging and gene expression profiles are emerging as a fundamental mechanism by which neurons adapt their transcriptional response to environmental cues (Feng *et al.* 2007; Sweatt 2009; Bousiges *et al.* 2010; Meaney and Ferguson-Smith 2010; Riccio 2010; Nelson and Monteggia 2011; Pirooznia and Elefant 2012). One of the best-characterized forms of epigenetic chromatin modification in the learning and memory field is histone acetylation (Peixoto and Abel 2013), which is regulated by the antagonistic activities of histone acetyltransferases (HATs) and histone deacetylases (HDACs) (Legube and Trouche 2003). Blocking histone acetylation has been reported to impair both long-lasting synaptic plasticity and behavioral performance (Korzus *et al.* 2004). Notably, inhibition of histone deacetylase activity reverses such deficits and improves memory formation (Korzus *et al.* 2004; Levenson *et al.* 2004), thus highlighting the importance of histone acetylation for memory formation.

Disruption of epigenetic gene control mechanisms in the brain causes significant cognitive impairment that is a debilitating

doi: 10.1534/genetics.114.171660
Manuscript received July 23, 2014; accepted for publication October 13, 2014; published Early Online October 17, 2014.
Supporting information is available online at http://www.genetics.org/lookup/suppl/doi:10.1534/genetics.114.171660/-/DC1.
[1]Corresponding author: Drexel University, 3141 Chestnut St., Philadelphia, PA 19104. E-mail: fe22@drexel.edu

hallmark of most neurodegenerative disorders, including Alzheimer's disease (AD). Sporadic cases of reduced histone acetylation levels are found in the brains of animal models for multiple types of neurodegenerative diseases that include AD. These changes have been shown to cause an epigenetic blockade of transcription that results in cognitive impairment. (Graff *et al.* 2012a). Pharmacological treatments aimed at increasing histone acetylation levels by inhibiting histone deacetylase action in these models have shown promising effects in reversing cognitive deficits (Kazantsev and Thompson 2008). However, little is known about HATs that modify the neural epigenome by laying down specific epigenetic marks required for proper cognition and thus likely serve as causative agents of memory-impairing histone acetylation changes. A promising candidate is the HAT, Tip60 (Tat interactive protein), which has been implicated in AD owing to its role in epigenetically regulating gene expression via complex formation with the amyloid precursor protein (APP) intracellular domain (AICD) (Cao and Sudhof 2001, 2004).

Tip60 is a multifunctional HAT that has been shown by others and us to epigenetically regulate genes essential for neurogenesis (Lorbeck *et al.* 2011; Pirooznia *et al.* 2012b). Such an effect is thought to be mediated through recruitment of Tip60-containing protein complexes to target gene promoters in the nervous system that are then epigenetically modified via site-specific acetylation and accordingly activated or repressed. We have recently reported that the histone acetylase function of Tip60 promotes neuronal and organismal survival in a *Drosophila* model for AD by activating pro-survival factors while concomitantly repressing activators of cell death (Pirooznia *et al.* 2012b). Overexpression of Tip60 also promotes axonal growth of the *Drosophila* circadian neurons, the small ventrolateral neurons (sLNvs), and rescues axonal outgrowth and transport as well as associated behavioral phenotypes such as sleep and locomotion under APP-induced neurodegenerative conditions (Pirooznia *et al.* 2012a). While these effects support a neuroprotective role for Tip60 under degenerative conditions such as those induced by neuronal overexpression of APP, an epigenetic role for Tip60 in mediating gene expression changes that underlie memory formation remains to be elucidated.

Drosophila is an attractive model for studies focused on molecular dissection of components of memory formation due to the availability of reproducible memory assays and genetic tools that enable restricting gene expression manipulation to specific subregions of the brain (Siwicki and Ladewski 2003; Fiala 2007; Kahsai and Zars 2011). The *Drosophila* mushroom body (MB) is known to regulate behavioral and physiological functions that range from olfactory learning and courtship conditioning to decision making under uncertain conditions (Heisenberg 2003; Margulies *et al.* 2005; Akalai *et al.* 2006; Farris 2013; Guven-Ozkan and Davis 2014). Courtship conditioning in *Drosophila* is a complex behavioral learning paradigm that requires multimodal sensory input involving chemosensory, mechanosensory, visual, and olfactory pathways and is thus well suited to study experience-dependent synaptic plasticity (Dubnau and Tully 2001; Mehren *et al.* 2004; Keene and Waddell 2007; Busto *et al.* 2010).

In this study, we focus on the *Drosophila* MB as a well-characterized cognition model to investigate an epigenetic role for Tip60 HAT action in learning and memory formation. We find that Tip60 is robustly produced in the MB of the adult fly brain. Targeted loss of Tip60 HAT activity in the MB causes abnormal development of the MB axonal lobes, while increasing Tip60 HAT levels causes no morphological defects. Furthermore, we show that misregulation of Tip60 HAT activity in the MB leads to immediate-recall memory deficits in adult flies. Our ChIP-Seq analysis reveals that Tip60 target genes are enriched for functions in cognitive processes, and, accordingly, key genes representing these pathways are misregulated in the Tip60 HAT mutant fly brain. Importantly, we show that both learning and memory defects in *Drosophila* that occur under AD-associated, APP-induced neurodegenerative conditions can be effectively rescued by increasing Tip60 HAT levels in the *Drosophila* MB. Together, our studies uncover an epigenetic transcriptional regulatory role for Tip60 HAT action in cognitive function and highlight the therapeutic potential of utilizing specific HAT activators for treatment of cognitive deficits in neurodegenerative disorders.

Materials and Methods

Fly stocks and maintenance

Flies were reared on standard medium (cornmeal/sugar/yeast) at 25° with a 12-hr light/dark (LD) cycle. Canton-S flies were used as wild-type controls. OK107-GAL4 and UAS-GFP stocks were obtained from the Bloomington *Drosophila* Stock Center (Indiana University). The generation and characterization of UAS-dTip60^{E431Q} and UAS-dTip60^{WT} flies are described in Lorbeck *et al.* (2011). Generation and characterization of the double-transgenic UAS-Tip60;APP fly lines are described in Pirooznia *et al.* (2012b). Double-transgenic lines carrying the UAS-mCD8-GFP and either UAS-dTip60^{E431Q} or UAS-dTip60^{WT} constructs were generated according to standard procedures. All of the UAS-dTip60 fly lines described here are contained within a w^{1118} genetic background. Additionally, for all experiments, transgene expression levels for each of the UAS fly lines were assessed as described (Lorbeck *et al.* 2011; Pirooznia *et al.* 2012a,b; Johnson *et al.* 2013) to ensure that the different transgenic lines used for phenotype comparisons show equivalent dTip60^{E431Q}, dTip60^{WT}, APP, or APP-CT expression levels.

Courtship suppression assay

Assays were performed as described in McBride *et al.* (2005) and Melicharek *et al.* (2010). Briefly, virgin males of the appropriate genotype were collected within 6 hr of eclosion and reared in individual food vials at 25° in 12:12 LD for

5 days prior to behavioral training and testing. Virgin wild-type Canton-S females were collected and kept in groups in food vials. Mated Canton-S females used for training were 5 days old and observed to have mated with a Canton-S male the evening prior to training. Virgin Canton-S females used for testing were 5 days old. All experiments were conducted during light phase. All behavior was digitally recorded using a Sony DCR-SR47 Handycam with Carl Zeiss optics. The total time that a male performed courtship activity was subsequently measured and scored. The courtship index was calculated as the total time observed performing courting behavior divided by the total time assayed.

On the day of training (day 5), male flies were assigned to random groups, and the assay set up with the experimenter blind to the genotype of the test males. Male flies were transferred without anesthesia to one half of a partitioned mating chamber from Aktogen (http://www.aktogen.com) that contained a previously mated Canton-S female in the other partitioned half. Males were allowed to acclimate for 1 min, and then the partition between the male and female was removed. Male flies were then trained for 60 min. After 60 min, male flies were transferred within 2 min without anesthesia to one half of a clean partitioned mating chamber that contained a virgin Canton-S female in the other partitioned half. The partition was removed, and behavior of the flies was recorded for 10 min. During the testing phase, untrained males of the appropriate genotype were assayed alongside the trained males to serve as controls. To determine the significance between different measures of the same genotype, a two-tailed paired Student's *t*-test was performed. Significance was determined at the 95% confidence interval.

Immunohistochemistry and antibodies

Third instar larvae or adult brains were dissected in PBS, fixed in 4% paraformaldehyde in PBS, washed three times in PBS containing 0.1% Triton X-100, blocked for 1 hr at room temperature (RT) in PBT containing 5% normal goat serum, and incubated with primary antibodies in blocking solution overnight at 4°. Anti-Tip60 (1:400) was generated by Open Biosystems (Rockford, IL), and anti-Fasciclin (mAb1D4; 1:10), anti-Trio (mAb9.4A; 1:4), anti-ELAV (1:400) were obtained from the Developmental Studies Hybridoma Bank (University of Iowa). Anti-GFP (1:100) was obtained from Millipore. Samples were washed three times in PBT at RT, and secondary antibodies (Jackson Immunoresearch) were applied in blocking solution for 2 hr at RT. After washing three times in PBS, samples were mounted in Vectashield (Vector Laboratories).

Imaging and quantification

Larval and adult brain preparations were imaged using the appropriate secondary antibodies. Anti-GFP and anti-Tip60 immunostaining were visualized using Alexa-Fluor 488 and Alexa-Fluor 647, respectively. Anti-Elav, anti-Fasciclin, anti-Trio were visualized using Alexa-Fluor 568. Confocal microscopy was performed using an Olympus microscope with fluoview acquisition software (Olympus, Center Valley, PA). Images were displayed as projections of 1-μM serial Z-sections. Consecutive subsets of the Z-stacks were utilized for the final projection. Images were adjusted for brightness and contrast using the ImageJ program to more clearly define MBs. Projections from unprocessed images are found in Supporting Information, Figure S1. Area of the MB lobes in the different genotypes was measured using National Institutes of Health ImageJ software.

Real-time PCR analysis

Total RNA was isolated from adult fly heads using the RNeasy Plus Mini Kit (QIAGEN). Complementary DNA (cDNA) was prepared using the SuperScript II reverse transcriptase kit (Invitrogen) according to the manufacturer's instructions with 1 μg total RNA and 0.2 μg/ml random hexamer primers (Roche Applied Science). PCRs were performed in a 20-μl reaction volume containing cDNA, 1 μM Power SYBR Green PCR Master Mix (Applied Biosystems), and 10 μM of both forward and reverse primers (primer pairs available upon request). PCR was performed using an ABI 7500 Real-Time PCR system (Applied Biosystems) following the manufacturer's instructions. Fold change in messenger RNA expression was determined by the ΔΔCt method.

Cell culture

Drosophila S2 cells (Invitrogen) were grown at 22° in Schneider's *Drosophila* Medium (Invitrogen) supplemented with 10% heat-inactivated fetal bovine serum (SAFC Biosciences, Lenexa, KS) and penicillin–streptomycin (Invitrogen)

ChIP-Seq

Chromatin from S2 cells was prepared as follows. Protein from 1–5 $\times$ 10^7 cells was cross-linked to DNA using 1% formaldehyde for 10 min at room temperature. Cross-linking was quenched by adding 2.5 M glycine to a final concentration of 0.125 M. Quenching was performed at RT for 10 min with constant agitation. The cells were then pelleted by centrifugation for 10 min at 2500 $\times$ *g* at 4°. The cells were washed with 1 ml of 1$\times$ PBS and pelleted by centrifugation for 10 min at 2500 $\times$ *g* at 4°. The pellet was then resuspended in 1 ml of cell lysis buffer supplemented with 5 μl each of protease inhibitor cocktail (PIC) and PMSF. The cells were transferred to an ice-cold douncer and dounced on ice to aid in release of nuclei. Lysed cells were transferred to a 1.7-ml centrifuge tube and centrifuged for 10 min at 5000 $\times$ *g* at 4° to pellet the nuclei. The supernatant was removed and the pelleted nuclei were resuspended in 350 μl of Shearing Buffer supplemented with 1.75 μl each of PIC and PMSF. The nuclei were sonicated at 30% output using a sonic dismembrator (Fischer Scientific, Pittsburgh) on ice for 40 sec. Sonication was carried out for a total of three times with 2-min intervals on ice yielding sheared chromatin fragments ranging from 200 to 500 bp.

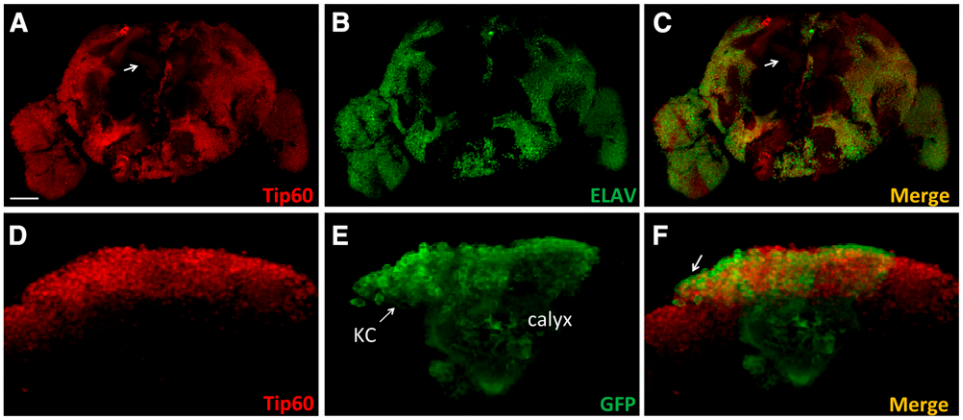

Figure 1 Tip60 expression in the adult *Drosophila* brain. Frontal view of a wild-type (Canton S) adult *Drosophila* brain stained with an antibody to Tip60 (red) and counterstained with anti-ELAV antibody (green). Tip60 is widely expressed in the adult fly brain (A) including the MB lobes (A, arrow), with an expression pattern similar to the pan-neuronal ELAV protein (B and C). (A–C) Whole-brain reconstruction of individual confocal image slices. Bar, 100 μM. A single confocal plane through the MB at the level of the calyx (approximately the center of the Z-stack) in flies that express mCD8-GFP under the control of OK107-GAL4 driver shows Tip60 expression in Kenyon cell (KC) nuclei with a halo of GFP expression in the cell membrane and calyx (dendritic processes) (D–F).

Chromatin precipitation assays were performed using a ChIP-IT Express Kit (Active Motif), following the manufacturer's instructions. Briefly, chromatin immunoprecipitation (ChIP) was carried out with 50 μg of sheared chromatin using three different antibodies: (i) 10 μg of RNA Pol II antibody (Abcam, Cambridge, MA); (ii) 10 μg of Tip60 antibody that targets residues 450–513 in the C terminus of Tip60 (Abcam); and (iii) 10 μg of Tip60 antibody that targets residues 500–513 in the C terminus of Tip60 (Thermo Fisher Scientific, Huntsville, AL). A mock reaction containing all reagents except the antibody was also set up as a control. The chromatin was immunoprecipated using the ChIP IT Express kit (Active Motif) exactly following the manufacturer's specifications. The eluted material from the immunoprecipitation was then purified using a QIAquick PCR purification kit (Qiagen) and was directly used for real-time PCR.

DNA library preparation and sequencing of ChIP DNA samples was carried out by the Jefferson Kimmel Cancer Center, Cancer Genomics Shared Resource. Sequencing of ChIP DNA samples was performed using the Illumina HiSeq2000 platform.

Bioinformatic analysis

Peak calling: MACS v1.4 peak-calling algorithm was used to find overrepresented sequence regions (peaks) representing likely *in vivo* binding sites for Tip60 or RNA Pol II, and the final set of significant peaks was produced in interval (BED) format. Prior to peak calling, BAM files of biological replicates for each antibody or input were merged together. Peak calling with MACS was done using the online Galaxy platform with the following parameters: mfold = 5, tag size = 35 nt, *P*-value cutoff = 1*e*-05, genome size = 130*e*+06, and FutureFDR = true.

Gene annotation of ChIP-Seq peaks: ChIP-Seq peaks in the form of genomic intervals (BED file) were intersected with genomic coordinates of genes in the *Drosophila melanogaster* genome annotation release R5.56 (ftp://ftp.flybase.net/releases/FB2014_02/) using the Galaxy platform (http://usegalaxy.org/), and gene identifiers were confirmed and converted where necessary for further analysis using the University of California at Santa Cruz (UCSC) table browser (http://genome.ucsc.edu/).

Functional annotation and cluster enrichment: Functional annotation and enrichment cluster analysis of the Tip60-associated gene list was performed using the Database for Annotation, Visualization and Integrated Discovery (DAVID) v6.7 and Gene Annotation Co-occurrence Discovery (GeneCodis) v3 (http://genecodis.cnb.csic.es/). *P*-values for significant enrichment were obtained with a hypergeometric test and corrected for multiple comparisons by FDR. Pathway enrichment was determined using the pathway enrichment module of the FlyMine integrated genomics database platform.

Tissue-specific expression profiles: Tissue-specific expression data for the 321 Tip60-associated genes were obtained from FlyAtlas using the FlyMine integrated genomics database.

Transcription factor motif enrichment: Transcription factor (TF) motif enrichment analysis was performed on Tip60-associated neuronal genes using the MEME-ChIP suite, RSAT (Thomas-Chollier *et al.* 2011, 2012), and Motif Enrichment Tool. TF motif databases utilized for comparison with discovered motifs included JASPAR Core Insects, FlyFactorSurvey, DMMPMM, and IDMMPMM *Drosophila* databases. As each tool employs a different algorithm for determining significance of motif enrichment and database match, where database matches are identified by more than one tool, significance values reported in this work represent the most conservative significance value found.

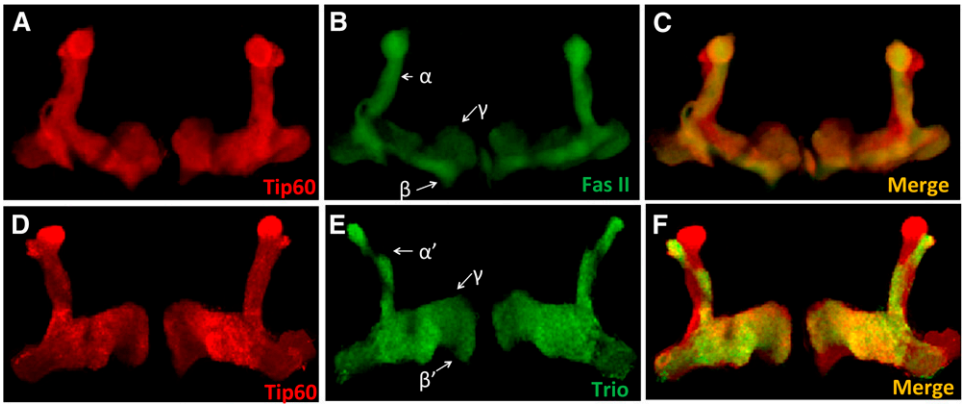

Figure 2 Tip60 is expressed in the MB lobes. Representative confocal images of adult MB lobes in wild-type (Canton S) *Drosophila* brain stained with Tip60 antibody (A and D) and costained with antibodies to either Fasciclin II (Fas II) (B) or Trio (E) antibodies. Fas II is a cell adhesion molecule that is expressed strongly in the MB α/β lobes and weakly in the γ lobe. Trio is a Dbl family protein that activates Rho family GTPases and is expressed strongly in the α′/β′ lobes and weakly in the γ lobe. Tip60 is expressed in all the lobes of the MB and colocalizes with Fas II and Trio in the α/β (C) and α′/β′ (F) lobes, respectively. Tip60 also colocalizes with Fas II and Trio in the γ lobes (C and F).

Results

Tip60 is expressed throughout the adult fly brain, including the mushroom body

Given the importance of brain-specific histone acetylation profiles in cognitive function, we wanted to examine whether the HAT Tip60 was produced in the adult fly brain. Tip60 production in the adult fly brain was characterized by immunohistochemistry on whole-mount Canton-S adult brains using an anti-*Drosophila* Tip60 antibody. We found that Tip60 was robustly and widely produced throughout the adult brain in a pattern similar to the pan-neuronal ELAV protein including the MB lobes (Figure 1, A–C). To examine Tip60 concentration in the MB, immunohistochemistry for Tip60 was performed on brains expressing mCD8-GFP under control of the MB-specific driver OK107-GAL4 that marks MB structure. In the MB neurons, called Kenyon cells, mCD8-GFP was observed in the cytoplasm surrounding the Tip60-positive nuclei and Tip60 was detected in all cells that expressed mCD8-GFP (Figure 1, D–F).

During development, the Kenyon cells of the MB undergo an ordered differentiation process into three types of neurons, namely, the α/α′ neurons, β/β′ neurons, and γ neurons (Lee *et al.* 1999). Each neuron projects dendrites that contribute to a large dendritic field in the calyx and an axon that travels anteroventrally, forming a tightly bundled peduncle before branching dorsally to form the α/α′ lobes and medially to form the β/β′ and γ lobes. In addition to the Kenyon cells, Tip60 was also detected in the α/α′, β/β′, and γ lobes (Figure 2, A and D). Specific MB lobes were unambiguously identified immunohistochemically by costaining with markers specific for each of the lobes. Fasciclin II (Fas II) is a cell adhesion molecule that participates in axonal pathfinding (Fushima and Tsujimura 2007) and is expressed strongly in the α/β lobes (Figure 2B) (Crittenden *et al.* 1998). *Drosophila* Trio is a Dbl family protein that participates in patterning of axons by regulating their directional extension and is expressed strongly in the α′/β′ lobes (Figure 2E) (Awasaki *et al.* 2000). Both markers are produced weakly in the γ lobe as well (Figure 2, B and E) (Bates *et al.* 2010). Tip60 production pattern in the α/β and α′/β′ lobes followed the pattern of Fas-II and Trio, respectively (Figure 2, C and F).

Appropriate Tip60 HAT levels are required for immediate-recall memory

Our finding that Tip60 is endogenously and robustly produced in the adult MB prompted us to ask whether Tip60 epigenetically regulates memory formation. To address this question, we used the conditioned courtship suppression assay (Siegel and Hall 1979). This assay is an associative conditioning procedure that measures both learning and memory in individual flies (Broughton *et al.* 2003). The conditioning aspect of the assay is based on the observation that male courtship behavior is modified by exposure to a previously mated female that is unreceptive to courting (Siegel and Hall 1979; Siwicki *et al.* 2005). Thus, after a 1-hr training session with a mated female, wild-type males suppress their courtship behavior even toward subsequent receptive virgin females, an effect that decays after 1–3 hr (Siegel and Hall 1979)

To examine the effect of Tip60 HAT function on learning and memory, we misregulated *Drosophila* Tip60 in the mushroom body by utilizing our previously reported transgenic lines that carry GAL4-responsive transgenes for either a dominant negative HAT defective version of dTip60 ($dTip60^{E431Q}$) or wild-type dTip60 ($dTip60^{WT}$) (Siegel and Hall 1979; Lorbeck *et al.* 2011). Expression of the respective transgenes was achieved continuously during development using the GAL4 driver OK107. This driver is expressed in discrete neuronal populations in the adult fly brain that includes high expression in the Kenyon cells, the intrinsic neurons of the MB, and the pars intercerebralis, suboesophageal ganglion, and optic lobes (Aso *et al.* 2009). To determine the effects on learning, male flies were placed in a courtship chamber with a previously mated (unreceptive) wild-type female for 60 min. The amount of time the male spent performing courtship behavior was assessed during the initial 10 min of this training and compared with the final 10 min of the training period. Male control flies (OK107-GAL4/+) show a significant drop in courtship behavior in the final 10 min of training when compared with

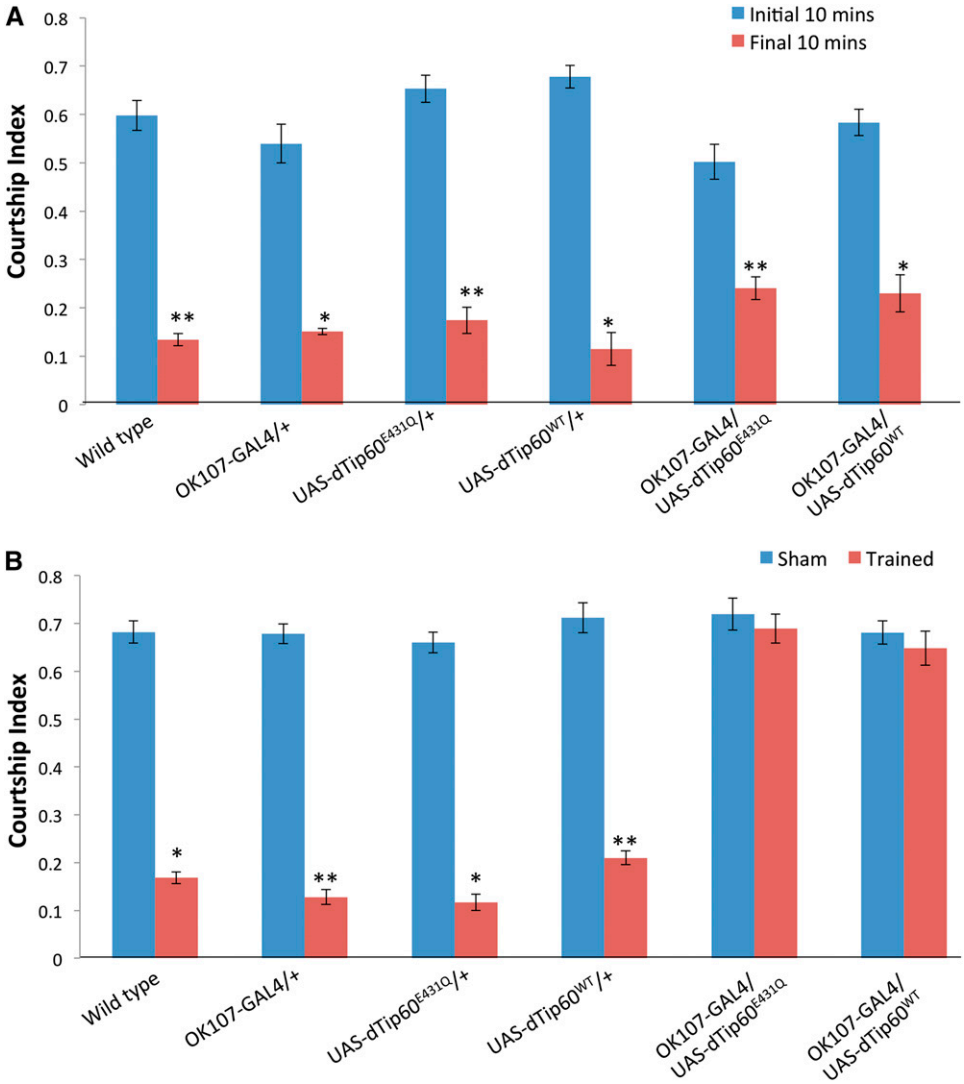

Figure 3 Misregulation of Tip60 in *Drosophila* MB does not affect learning but leads to defects in immediate-recall memory. (A) Learning during the initial 10 min (blue columns) and final 10 min (red columns) of the training phase during the courtship suppression assay. Genotypes are indicated. Flies expressing either the mutant Tip60 defective in its HAT activity ($dTip60^{E431Q}$) or additional copies of $dTip60^{WT}$ exhibit a marked decrease in courtship index during final 10 min compared to the initial 10 min, indicative of normal learning response. This is comparable to the response observed in wild type (Canton S) flies as well as in the corresponding GAL4 and UAS background controls. (B) Immediate-recall memory (0–2 min post-training) of trained males compared to untrained (sham) males of the same genotype. $dTip60^{E431Q}$ and $dTip60^{WT}$ flies show no significant difference between trained and sham males, indicative of no immediate recall of training. Error bars represent 95% confidence interval. In A, a single asterisk indicates $P < 0.05$ and a double asterisk indicates $P < 0.001$ compared with initial 10 min. In B, a single asterisk indicates $P < 0.05$ and a double asterisk indicates $P < 0.001$ compared with sham males. $n = 20$ for trained and untrained males in each genotype.

the initial 10 min (Figure 3A), indicative of an appropriate learning response. A similar effect was observed in the UAS background control flies (UAS-$dTip60^{E431Q}$/+ and UAS-$dTip60^{WT}$/+) and in the wild-type Canton-S flies (Figure 3A). Male flies expressing either the Tip60 HAT mutant ($dTip60^{E431Q}$) or additional copies of $dTip60^{WT}$ also showed a significant decrease in courtship behavior in the final 10 min of the training period compared with the initial 10 min (Figure 3A). This indicates that misregulation of Tip60 HAT activity in the MB does not interfere with the successful perception and interpretation of sensory stimuli required in this assay and that these flies are capable of altering their behavior appropriately (learn) in response to this training.

Different phases of memory have been defined in *Drosophila* and include immediate-recall memory (0–2 min post-training), short-term memory (up to 1 hr post-training), medium-term memory (up to 6 hr), anesthesia-resistant memory (up to 2 days) and long-term memory (up to 9 days) (Greenspan 1995; McBride *et al.* 1999, 2005). To test for the earliest phase of memory first, we assayed male flies expressing either the Tip60 HAT mutant ($dTip60^{E431Q}$) or $dTip60^{WT}$ by transferring the respective trained males to clean mating chambers and pairing with a receptive virgin female within 2 min of training, following which their courtship behavior was monitored for 10 min. Trained male control flies (OK107-GAL4/+) showed a marked decrease in their courtship activity compared to untrained male flies (Sham) that were assayed in parallel (Figure 3B). A similar effect was observed in the UAS background control flies (UAS-$dTip60^{E431Q}$/+ and UAS-$dTip60^{WT}$/+) and in the wild-type Canton-S flies (Figure 3B). This indicates a change in behavior in these flies that is consistent with normal immediate-recall memory training. However, such a decrease in courtship behavior was not observed in flies expressing either the Tip60 HAT mutant ($dTip60^{E431Q}$) or additional copies of the HAT competent $dTip60^{WT}$ (Figure 3B). Since these flies were capable of normal sensory perception and were also able to alter their behavior in response to their experience during the learning component of the assay, their inability to effectively suppress courtship behavior during the second

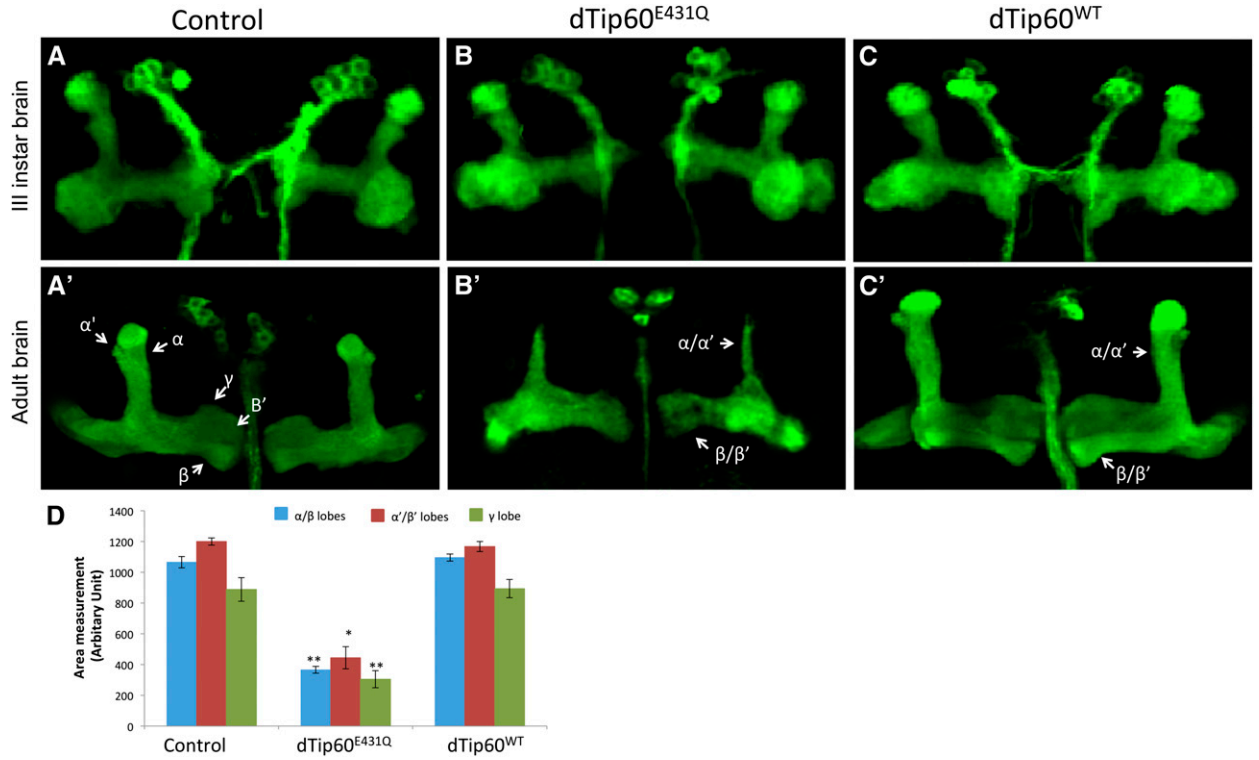

Figure 4 Tip60 is required for normal structures of the adult MB. Representative confocal images of larval and adult MB visualized with mCD8-GFP driven by the pan-MB driver OK107-GAL4. Images were displayed as projections of 1-μM serial Z- sections and were adjusted for brightness and contrast using the ImageJ program to more clearly define the MBs. Unprocessed images are shown in Figure S1. Third instar larval brain in control flies (A). Flies expressing mutant Tip60 defective in its HAT activity (dTip60^{E431Q}) (B) or additional copies of dTip60^{WT} (C) show no effect on MB structure in the third instar larva. GFP labeling shows similar widths of and α/β lobes in (A′) adult control brains (OK107-GAL4; UAS-GFP), whereas adult flies expressing mutant dTip60^{E431Q} display severe reduction in length and width of both α and β lobes (arrows) (B′) while overexpressing dTip60^{WT} did not have any effect on the MB in the adult flies (C′). (D) Quantification of area in the different genotypes in adult flies. MBs stained with GFP to delineate MB structure were counterstained with either Fas II staining (Figure 5) for quantification of area of α/β and γ lobes or Trio staining (Figure 6) for quantification of area of α′/β′ lobes where $n = 20$. Error bars represent 95% confidence interval. A single asterisk indicates $P < 0.05$, and a double asterisk indicates $P < 0.001$ compared to the respective MB lobes in the control.

component of the assay indicates that these flies are defective in immediate-recall memory of this form of learning.

Tip60 HAT activity is required for formation of normal MB structure in adult brains

Development of precise axonal connectivity and plasticity in their connectivity are required for maintenance of functional neural circuits that facilitate learning and memory (Luo and O'Leary 2005). Accordingly, degeneration of neural circuits essential for learning and memory may lead to impaired behavioral plasticity. We have previously reported that Tip60 HAT function promotes axonal growth of the *Drosophila* sLNv, a well-characterized model system for axonal growth (Pirooznia *et al.* 2012a). We therefore wanted to examine if the observed memory deficits in the Tip60 mutant flies were accompanied by axonal growth defects in the MB. To examine the Tip60-mediated anatomical effects in the MB, we generated GAL4-responsive transgenic fly lines carrying a membrane-bound mCD8-GFP construct with either the dominant negative Tip60 HAT mutant (UAS-mCD8-GFP; UAS-dTip60^{E431Q}) or wild-type Tip60 (UAS-mCD8-GFP; UAS-dTip60^{WT}). Expression of the respective transgenes was directed by the MB-specific OK107-GAL4 driver. MB structural phenotypes under the different conditions were identified by immunostaining for GFP in whole brains dissected from adult animals.

In the third instar larvae and adult control flies (OK107-GAL4/US-GFP), confocal microscopy revealed GFP immunolabeling of α/β neurons along the peduncles as well as distally as their axons bifurcate and project dorsally into the α/α′ lobes and medially into the β/β′ and γ lobes (Figure 4, A and A′). While the stereotyped morphology of the MB lobes was detected in third instar brain of flies expressing either the HAT mutant dTip60^{E431Q} or dTip60^{WT} (Figure 4, B and C), severe axonal defects were observed in the adult flies. GFP staining of adult brains from the dTip60^{E431Q} mutants revealed dramatic reduction of the MB axonal fields, resulting in α/α′ lobes that were much thinner than those in the control flies (Figure 4, B′ and D). Additionally, severe reduction in the area of the β/β′ and γ lobes was also observed in these flies (Figure 4, B′ and D). Thinner α and β lobes were observed in both sides of the brain in the dTip60^{E431Q} mutants, indicating that the axonal defects are common to both brain hemispheres. Developing axons of α/β neurons normally bifurcate at the base of the lobes, and the resulting sister

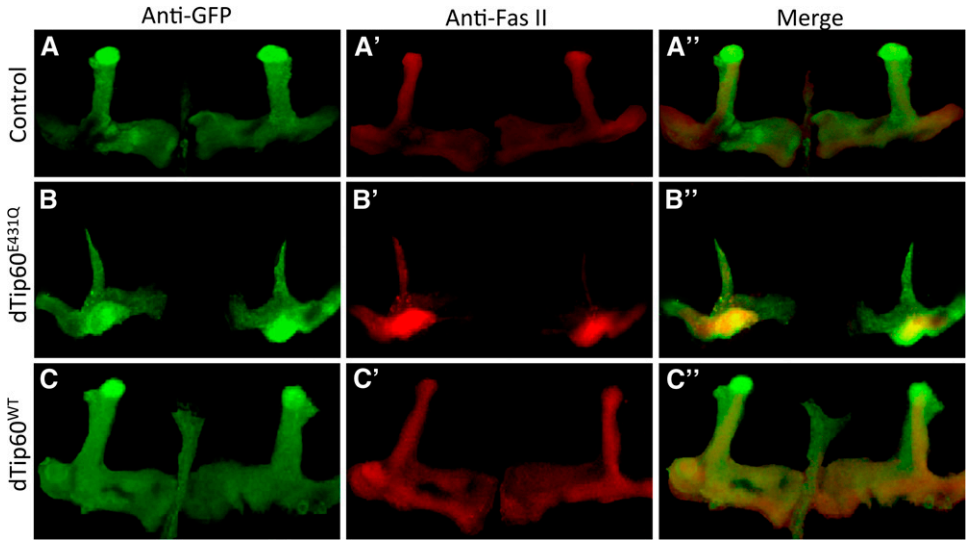

Figure 5 Fasciclin II labeling in the MB. Representative confocal images of OK107-GAL4 driver carrying a GFP construct was used to drive expression of dTip60^{E431Q} or dTip60^{WT}, and the effect on (A, B, C) MB structure was visualized using GFP and Fas II staining (A′, B′, C′) and co-staining of GFP and FasII (A″, B″, C″). Images were displayed as projections of 1-μM serial Z-sections and were adjusted for brightness and contrast using the ImageJ program to more clearly define MBs. Unprocessed images are shown in Figure S1. Compared to control brains (UAS-mCD8-GFP; OK107-GAL4), dTip60^{E431Q} flies exhibit a marked decrease in α/β and γ lobes while dTip60^{WT} flies did not exhibit any effects on α/β and γ lobes. Fas II labeling was used for quantifying area measurements in the different genotypes.

branches subsequently extend in diverging directions: one dorsally to the α lobe and the other medially to the β lobe. Similarly, α′/β′ neurons also develop dorsal (α′) and medial (β′) lobes. While the defects that we observed were present in all of the dTip60^{E431Q} MBs that we inspected, in some MBs the defects were more severe than in others. Therefore, to more accurately quantify the changes as well as to examine which particular lobe(s) were specifically affected in the dTip60^{E431Q} flies, area measurements of the different MB lobes were carried out by costaining with anti-Fas II or anti-Trio antibodies that exhibit weak expression in the γ lobe while strongly labeling α/β and α′/β′ lobes, respectively. Fas II staining (Figure 5, B and B′) was used for quantification of α/β and γ lobes, and Trio staining (Figure 6, B and B′) was used for quantification of the area of α′/β′ lobes. Quantification using these lobe-specific markers revealed a marked decrease in the area of all the MB lobes in the dTip60^{E431Q} flies compared to the control flies (OK107-GAL4; UAS-GFP) (Figure 4D). On the contrary, adult brains from the dTip60^{WT} flies did not exhibit any significant effect on α/β, α′/β′, and γ lobes on either side of the brain as revealed by GFP (Figure 4, C′ and D), Fas II (Figure 5C′), and Trio labeling (Figure 6C′). Thus, production of Tip60 within the MB lobes and the axonal growth defects observed due to disruption of Tip60's HAT function together suggest that Tip60 HAT activity may play essential roles in MB axonal outgrowth.

Tip60-associated target genes are enriched for functions in cognition-linked neuronal processes

Our prior findings demonstrated that gene control is a key mechanism by which Tip60 exerts its action in promoting function in a variety of neuronal processes. To determine whether Tip60 associates with target genes enriched for cognition-linked processes, we conducted genome-wide analysis of Tip60 occupancy using ChIP-Seq analysis. We also carried out ChIP-Seq analysis for the transcriptionally active elongation version of RNA polymerase II occupancy to assess which Tip60-associated gene targets were transcriptionally active. To identify early developmental targets, we used the *Drosophila* S2 embryonic cell line that robustly produces endogenous Tip60 (Zhu *et al.* 2007) and is composed of mixed cell types for an unbiased enrichment analysis.

To identify Tip60-associated target genes, gene annotation of Tip60 and RNA Pol II ChIP-Seq peaks was performed using the *D. melanogaster* annotation database R5.5 and UCSC table browser, producing a list of 321 gene targets for Tip60 and 2210 for RNA Pol II. Functional annotation clustering analysis was performed on the list of 321 Tip60-associated genes using both DAVID and GeneCodis3 (Tabas-Madrid *et al.* 2012). Analysis of these functional clusters (Figure 7A) revealed that they were enriched for a variety of neuronal processes all linked to cognition. Next, tissue-specific expression data for the 321 Tip60-associated genes was obtained through FlyAtlas. Figure 7B shows the percentage of Tip60-associated genes that are upregulated and downregulated in the various fly tissue types. Importantly, these data show that in neuronal tissues (brain, head, larval CNS, and thoracicoabdominal ganglion), ∼60–65% of Tip60 target genes are robustly expressed, while in other tissue types, the majority of Tip60 target genes show low-level expression. To produce a comprehensive list of Tip60-associated "neuronal genes," we combined the list of 46 neuronal genes identified through Gene Ontology functional annotation with additional Tip60-target genes that are upregulated in neuronal tissues relative to whole fly, as determined based on tissue-specific expression data from FlyAtlas. This produced a comprehensive list of 178 unique neuronal genes targeted by Tip60. Importantly, 132 of 178 neuronal genes targeted by Tip60 showed colocalization of RNA Pol II, suggesting that the majority of Tip60-target neuronal genes are actively transcribed (Figure 7C). Further analysis using the DAVID and Gene Codis3 classification system revealed that a substantial number of these genes were functionally linked to specific cognition-linked pathways (Table 1), many of which were activity-dependent signaling

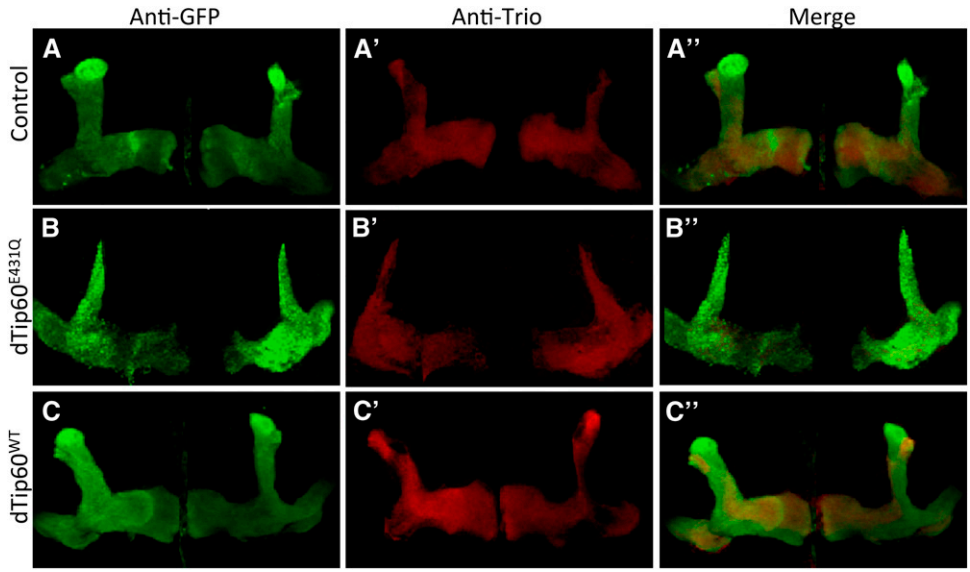

Figure 6 Trio labeling in the MB. Representative confocal images of OK107-GAL4 driver-carrying GFP construct was used to drive expression of dTip60^{E431Q} or dTip60^{WT}, and the effect on MB structure was visualized using GFP (A, B, C) and Trio staining (A′, B′, C′) and co-staining of GFP and Trio (A″, B″, C″). Images were displayed as projections of 1-μM serial Z-sections and were adjusted for brightness and contrast using the ImageJ program to more clearly define MBs. Unprocessed images are shown in Figure S1. Compared to control brains (UAS-mCD8-GFP; OK107-GAL4), dTip60^{E431Q} flies exhibit a marked decrease in α′/β′ while dTip60^{WT} flies exhibit no significant effects on α′/β′ lobes. Trio labeling was used for quantifying area measurements in the different genotypes.

pathways. Full lists of total Tip60 gene targets and neuronal Tip60 gene targets are shown in Table S1 and Table S2, respectively. To identify the enrichment of known transcription factor DNA-binding motifs within Tip60-target-gene intervals, a motif enrichment analysis was performed using the MEME-ChIP suite as well as RSAT and Motif Enrichment Tool. DNA recognition sequences and statistical significance for top hit TFs involved in various neuronal functions are shown in Figure S2.

Based on our ChIP-Seq analysis, we hypothesized that the memory disruption and MB morphological defects that we observed upon Tip60 HAT misregulation was caused by inappropriate expression of genes required for these processes. To test this hypothesis, we performed quantitative real-time PCR analysis of 10 genes identified in our ChIP-Seq analysis that were well-characterized representatives of a particular cognition-linked pathway, this time using adult fly heads expressing dTip60^{E431Q} under the control of the elav-GAL4 driver (Figure 8). Each of the 10 genes that we tested were significantly downregulated in response to Tip60 HAT. These genes included those required for axonal extension, guidance, and target recognition such as ben, brat, CadN2, and pyd, consistent with the MB axonal outgrowth defects that we observed in Tip60^{E431Q} mutant fly brains (Figure 4). Moreover, genes required for memory such as *rut*, *ptp10d*, and *fas2* as well as a core dendrite morphogenesis gene *chinmo* and the neurotransmitter release gene *aux* were also negatively affected, consistent with the memory defects that we observed in the Tip60^{E431Q} flies (Figure 3). Taken together, our findings support a transcriptional regulatory role for Tip60 HAT activity in the activation of genes essential for cognitive processes.

Increasing Tip60 levels in the MB of the fly CNS rescues learning and memory defects under APP-induced neurodegenerative conditions

We previously reported that Tip60 plays a neuroprotective role in AD neurodegenerative progression by demonstrating that increased levels of Tip60 HAT activity suppress AD deficits that include apoptotic-induced neurodegeneration, axonal outgrowth and transport defects, and associated sleep and locomotion behavioral phenotypes in a *Drosophila* model overexpressing APP (Pirooznia *et al.* 2012a,b; Johnson *et al.* 2013; Pirooznia and Elefant 2013b). Given the importance of histone acetylation in cognitive ability (Pirooznia and Elefant 2012; Peixoto 2013; Pirooznia and Elefant 2013a; Fischer 2014) and our finding that appropriate levels of Tip60 HAT activity are required for short-term memory (Figure 3, A and B), we hypothesized that excess Tip60 might also rescue AD-linked cognitive deficits. To test this hypothesis, we again used the conditioned courtship suppression assay to assess learning and memory, this time using a unique AD fly model generated in our laboratory that co-expresses equivalent levels of dTip60^{WT} or dTip60^{E431Q} with either APP or APP dCT (APP lacking the C terminus that forms the transcriptional regulatory Tip60/AICD complex) (Siegel and Hall 1979). We found that flies exhibited both learning and short-term memory defects when APP expression was targeted specifically to the fly MB using GAL4 driver OK-107 GAL4 and that these cognitive deficits were dependent upon the presence of the Tip60-interacting C terminus of APP. Remarkably, our studies revealed that excess levels of Tip60 in the fly MB rescued such APP-induced learning and memory defects (Figure 9, A and B) and that this rescue was dependent upon both a functioning Tip60 HAT domain and the Tip60-interacting C terminus of APP (Figure 9, A and B). (Gunawardena and Goldstein 2001; Merdes *et al.* 2004). Taken together, our results support a neuroprotective role for Tip60 HAT activity in APP-induced cognitive deficits associated with AD.

Discussion

Our previous work using a *Drosophila* model system demonstrated that Tip60 HAT function is critical for a variety of

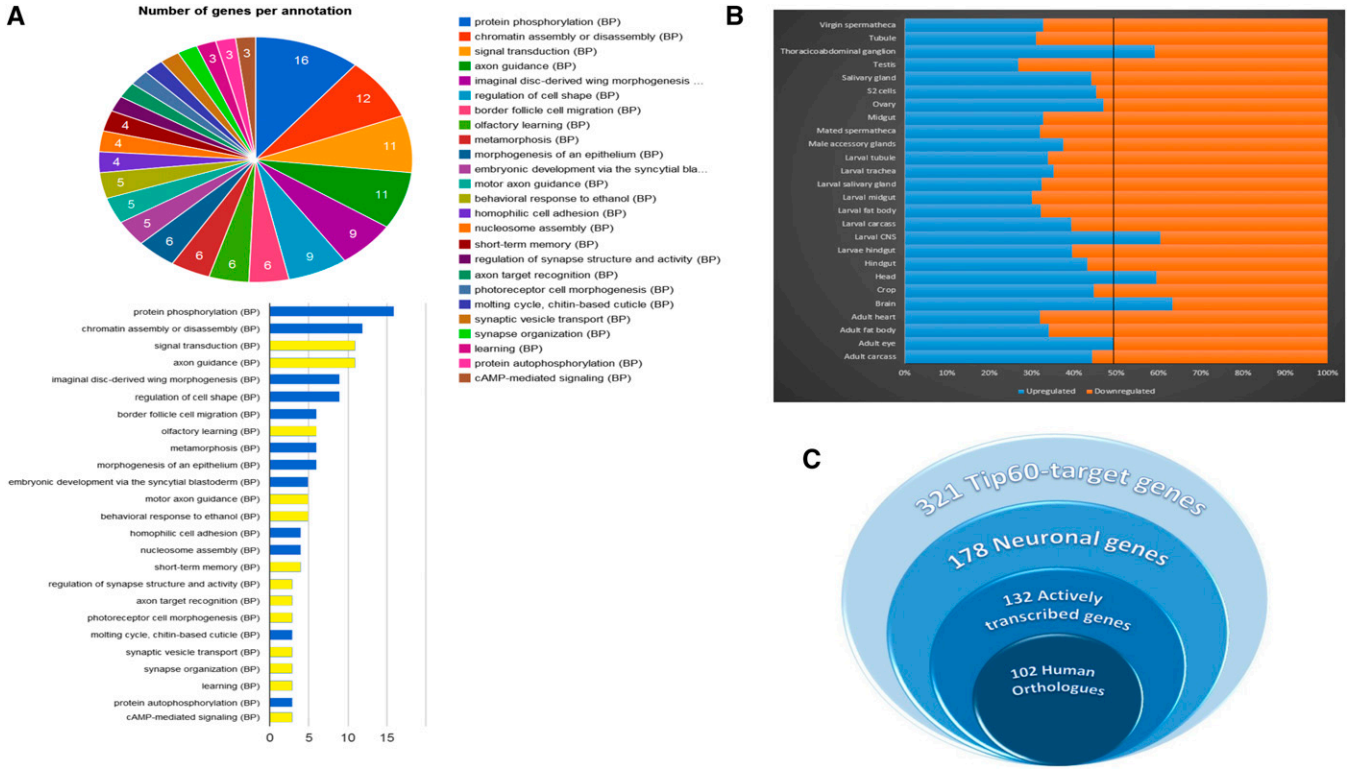

Figure 7 Tip60 associates with genes enriched for neuronal functions. (A) Functional annotation clustering of Tip60-associated genes using GeneCodis. Only clusters containing more than two genes and having significant enrichment are shown. (B) Tissue-specific expression profiles for Tip60-associated genes. Expression profiles were obtained through FlyAtlas. Histogram analysis depicts that the majority of Tip60-associated genes are robustly expressed specifically in tissues with neuronal function. (C) Proportions of different gene categories in Tip60-target genes. A total of 132 neuronal genes targeted by Tip60 showed colocalization of an active elongation version of RNA Pol II, suggesting that these Tip60-target neuronal genes are actively transcribed.

cognition-linked processes that include synaptic plasticity, axonal outgrowth and transport, and neuronal cell apoptotic control in the CNS (Sarthi and Elefant 2011; Pirooznia *et al.* 2012a,b; Johnson *et al.* 2013; Pirooznia and Elefant 2013a). Our present study extends these findings to demonstrate that Tip60 HAT activity plays an integral functional role in memory formation in *Drosophila*. Here, we show that loss of dTip60 HAT activity or increased levels of dTip60 HAT activity in all the lobes of the MB, the learning and memory center of the *Drosophila* CNS, disrupt immediate-recall memory while there is no effect on learning. In the dTip60^{E431Q} HAT mutant flies, memory defects are also accompanied by axonal growth defects that are evident in dorsal α/α′ and medial β/β′ and γ lobes of the adult MB in these flies with no marked effect on the larval MB structure. The α, β, and γ neurons composing the MB undergo considerable structural reorganization during embryonic, larval, and pupal development. The γ neurons are the earliest born and develop during first instar larval stages while development of α′/β′ axons and α/β axons takes place during the third instar larval and pupal stages, respectively (Scott *et al.* 2001). Although the α/β lobes appear much later in development than the α′/β′ lobes, the dramatic effects that we observe on both these lobes in the dTip60^{E431Q} adult flies indicate that Tip60 HAT activity may be crucial for development of α/β lobes as well as for maintaining branch stability in the larval-born α′/β′ lobes as development proceeds. During metamorphosis, the γ neurons undergo a stereotypical process of axon elimination wherein the dorsal and medial segments of its axon are pruned back (Watts *et al.* 2003, 2004). The γ axons subsequently re-extend medially during pupal remodeling. Tip60 HAT activity likely mediates regeneration of γ axons as well during pupal development as evidenced by the severe reduction of these axons in the adult flies that express the HAT-defective dTip60^{E431Q} mutant. Consistent with these findings, we recently reported a similar effect in the axons of *Drosophila* sLNv, a well-characterized model system for studying axonal growth, wherein Tip60 HAT loss inhibits sLNv axon outgrowth in the adult flies while no axonal defects were observed in the third instar larva (Pirooznia *et al.* 2012a). Together, these results support a role for Tip60 HAT activity in mediating MB axonal outgrowth required for proper adult MB axonal formation.

Transcription of genes involved in synaptic plasticity is a highly regulated process, and it is becoming increasingly clear that HATs and HDACs are key regulators in this process (Graff and Mansuy 2008; Sweatt 2009). As such, epigenetic PTMs of histone proteins, most notably histone acetylation, that control nuclear chromatin packaging and gene expression profiles are emerging as a fundamental mechanism by which neurons adapt their transcriptional response to environmental cues (Feng *et al.* 2007; Sweatt 2009; Bousiges

Table 1 Activity-dependent, cognition-linked pathways enriched for Tip60-associated genes

Pathway name	*P*-value	Gene count
Signaling pathways	0.033862	20
Signaling by GPCR, G-protein coupled receptor	0.000155	13
GPCR downstream signaling	0.00767	9
Integration of energy metabolism	0.018144	9
Neuronal system	0.025936	9
Signaling by NGF, nerve growth factor	0.028872	9
Axon guidance	0.022689	8
NGF signaling via TRKA, tyrosine kinase, from the plasma membrane	0.02838	8
Gα signaling events	0.024443	5
Activation of NMDA receptor upon glutamate binding and postsynaptic events	0.029943	4
PKA activation	0.039547	4
Ca-dependent events	0.039547	4
Calmodulin-induced events	0.039547	4
CaM pathway	0.039547	4

et al. 2010; Meaney and Ferguson-Smith 2010; Riccio 2010; Nelson and Monteggia 2011; Pirooznia and Elefant 2012). The implicit hypothesis is that environmental signals drive changes in histone acetylation modifications that are inherently dynamic in nature. Such changes allow for activity-dependent transcriptional "plasticity" that mediates sustained variation in neural function (Sweatt 2009; Riccio 2010; Graff *et al.* 2012b; Bousiges *et al.* 2013). One of the most important of such experience-driven behavioral changes is learning and memory formation, as it directly impacts cognitive ability (Levenson and Sweatt 2005; Carulli *et al.* 2011; Nelson and Monteggia 2011; West and Greenberg 2011). Importantly, the MB is a highly plastic brain region in the *Drosophila* CNS that is well known for its role in multimodal sensory integration and associative learning. Thus, it serves as a powerful model to study not only developmental synaptic reorganization but also experience-dependent, cognition-linked plasticity (Technau 1984; Heisenberg *et al.* 1995; Barth and Heisenberg 1997). Here we show that robust production of Tip60 is localized in the MB Kenyon cell nuclei. Moreover, our ChIP-Seq analysis reveals that Tip60 direct target genes are enriched for functions in cognitive processes and that key genes representing these pathways are misregulated in the adult Tip60 HAT mutant fly brain. We acknowledge that, because theTip60 target genes that we show here were identified in S2 cells, they cannot be assumed to be the same *in vivo*. However, our findings are consistent with our previous microarray study performed on Tip60 HAT mutant second instar larvae *in vivo* that showed misregulation of genes enriched for neuronal function (Lorbeck *et al.* 2011). Intriguingly, we found that many of the pathways enriched for Tip60-associated genes are activity dependent (Table 1). Taken together, our studies uncover an epigenetic transcriptional regulatory role for Tip60 HAT action in cognitive function and suggest that Tip60 function in gene control may rely on experience-driven modes of action.

Several other brain regions in addition to the MB have been identified to be important for courtship learning. Basic courtship involves communication between the projection neurons from the antennal glomeruli with higher centers in the lateral protocerebrum and MBs (Mehren *et al.* 2004). Recent studies using cobalt labeling and ectopic expression of the ATP receptor P2X2 in the MB Kenyon cells also suggest the existence of functional feedback from MBs to the antennal lobes, a process crucial for sensory processing (Rybak and Menzel 1993; Hu *et al.* 2010). Furthermore, such functional feedbacks from the Kenyon cells are thought to be mediated by the β and γ lobes (Hu *et al.* 2010), which are also severely affected in the dTip60^{E431Q} flies. Changes in neuronal connectivity in the CNS are also thought to contribute to behavioral defects in several *Drosophila* learning mutants that alter cAMP signaling (Guan *et al.* 2011). Thus, the axonal growth defects that we observe in the dTip60^{E431Q} flies may result in disruption of synaptic connectivity between the MB and neural circuits in the protocerebrum essential for sensory processing, subsequently leading to the observed memory impairment. Intriguingly, although overexpression of dTip60^{WT} did not have an observable effect on the MB structure *per se*, the dTip60^{WT}-expressing flies exhibit defects in immediate-recall memory similar to the dTip60^{E431Q} flies. Importantly, under normal conditions, maintaining the balance between HAT and HDAC levels and activity is critical for establishing proper histone modification patterns that serve to regulate both stable and rapidly changing gene expression profiles crucial for both neuronal homeostasis and appropriate neurophysiological response outputs such as long-term potentiation, learning, and memory, respectively (Morris 2003). Thus, we speculate that increasing Tip60-mediated acetylation in the MB can lead to complex changes in the chromatin landscape, causing misregulation of genes that are induced following patterned synaptic stimulation, such as behavioral experiences. Such changes play a critical role in translating the activity in neural circuits into accessible memories in the brain (Pirooznia and Elefant 2012, 2013a).

Outgrowth and stabilization of axons during development of the nervous system and reorganization of axonal connections in the adult in response to environmental cues critical for cognition are based on the dynamic rearrangement of the cytoskeleton (Baas and Luo 2001; Dent and Gertler 2003). Axon growth and elongation depends, among other factors, on microtubule polymerization (Conde and Caceres 2009), and acetylation of α-tubulin has been reported to stabilize microtubules and promote polymerization (Creppe *et al.* 2009). Accordingly, reducing levels of HDAC6 has been reported to restore learning and memory as well as α-tubulin acetylation in a mouse model for AD (Govindarajan *et al.* 2013). Consistent with these findings, we previously reported that Tip60 partially acetylates microtubules in the larval neuromuscular junction (NMJ), an effect that was dependent on its HAT function (Sarthi and Elefant 2011), although we did not observe this effect in

A

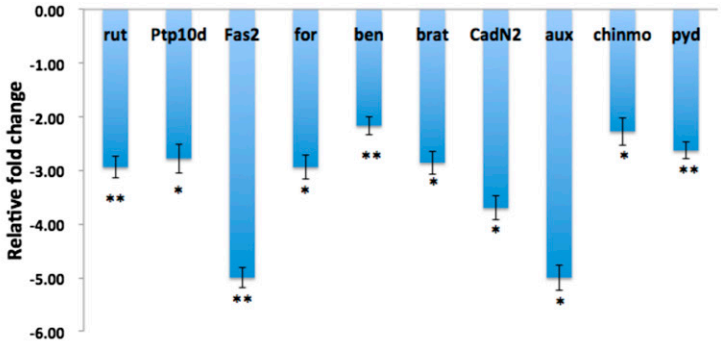

B

Gene Name	Common Name	qPCR Fold Change dTip60 ^{E431Q}	Phenotype/Disease	Inferred Function
rut	rutabaga	-2.94	sensory perception defective	membrane-bound calmodulin-sensitive adenylyl cyclase
Ptp10d	Protein tyrosine phosphatase 10D	-2.78	motor neuron axon guidance and central nervous system development defect	involved in axon outgrowth and guidance
Fas2	Fasciclin 2	-5	synapse organization and learning and memory defect	neuronal recognition molecule for the MP1 axon pathway
for	foraging	-2.94	short- and long-term memory defect	protein serine/threonine kinase activity
ben	benless	-2.17	axonogenesis defect	amino acid ligase activity
brat	brain tumor	-2.86	neurogenesis and brain development defect	growth suppressor involved in brain tumor suppression
CadN2	Cadherin-N2	-3.7	axon extension defect	calcium-dependent cell adhesion proteins.
aux	auxillin	-5	synaptic vesicle uncoating	protein serine/threonine kinase activity
chinmo	chronologically inappropriate morphogenesis	-2.27	dendrite morphogenesis and mushroom body developmental defect	metal ion binding
pyd	polychaetoid	-2.63	adherens junction strength	cell adhesion molecule binding

Figure 8 Tip60 HAT loss in the CNS causes misregulation of neuronal genes. (A) Real-time PCR was performed on cDNA isolated from adult fly heads expressing dTip60 ^{E431Q} under the elav C155 pan-neuronal GAL4 driver. Histogram represents relative fold change in expression level of neuronal target genes. Real-time PCRs were performed in triplicate, and the fold change was calculated using the ΔΔCT method. Statistical significance was calculated using an unpaired Student's *t*-test: $*P < 0.05$ and $**P < 0.01$. (B) List of selected learning- and memory-related genes and their functions that are identified in ChIP-seq analysis and validated in adult head tissue using quantitative RT-PCR.

motor neuron axons of the *Drosophila* CNS (Johnson *et al.* 2013). Here, our analysis reveals that Tip60 is localized not only within the nucleus of the Kenyon cells in the MB but also within all the MB axonal lobes, indicative of both nuclear and cytoplasmic localization for Tip60. Such cytoplasmic and nuclear Tip60 localization is recapitulated in the *Drosophila* NMJ, where we previously reported Tip60 to be localized both pre- and postsynaptically (Sarthi and Elefant 2011). Therefore, we cannot rule out the possibility that Tip60 may also mediate axonal growth by modulating cytoskeletal dynamics in the MB through direct binding and acetylation of cytoskeletal proteins that function to promote and stabilize axon growth. Notably, neural activity has been shown to modulate chromatin acetylation in hippocampal neurons in part by controlling the shuttling of certain HDACs in and out of the nucleus that, in turn, influences their activity in gene control (Chawla *et al.* 2003; Riccio 2010). Thus, Tip60 may also utilize a similar cytoplasmic/nuclear shuttling mechanism, an area that we are currently exploring.

Tip60 has been implicated in AD via its interaction with the AICD, a fragment generated by the processing of APP by γ-secretase that is subsequently released into the cytoplasm (Muller *et al.* 2008). AICD forms a transcriptional competent protein complex with the HAT Tip60 (Cao and Sudhof 2001) and is recruited to the promoters of specific neuronal target genes where it acts to acetylate select histone proteins to epigenetically regulate gene transcription (Cao and Sudhof 2001; Von Rotz *et al.* 2004; Ryan and Pimplikar 2005). Importantly, misexpression of certain Tip60/AICD target genes such as neprilysin, EGFR, LRP, and KAI-1 have been associated with AD pathophysiology (Baek *et al.* 2002; Muller *et al.* 2007; Slomnicki and Lesniak 2008). Based on these findings, it has been proposed that the inappropriate AICD/Tip60 complex formation and/or its recruitment may contribute or lead to AD pathology via epigenetic transcriptional misregulation of target genes required for neuronal functions (Pirooznia and Elefant 2012, 2013a; Johnson *et al.* 2013). Here, we report that, while misregulation of Tip60 HAT activity alone causes short-term memory deficits in the fly, excess production of Tip60 in conjunction with APP rescue both APP-induced learning and immediate-recall memory deficits in a fly model overexpressing APP. Importantly, reversal of these cognitive deficits is dependent upon the C terminus of APP that forms the transcriptional regulatory Tip60/AICD complex as well as the functional HAT activity of Tip60. Accordingly, we show by ChIP-Seq that Tip60-associated genes are enriched for cognition function and that key Tip60 genes representing learning- and memory-linked pathways are misregulated in the Tip60 HAT mutant fly brain *in vivo*. Consistent with these findings, we previously

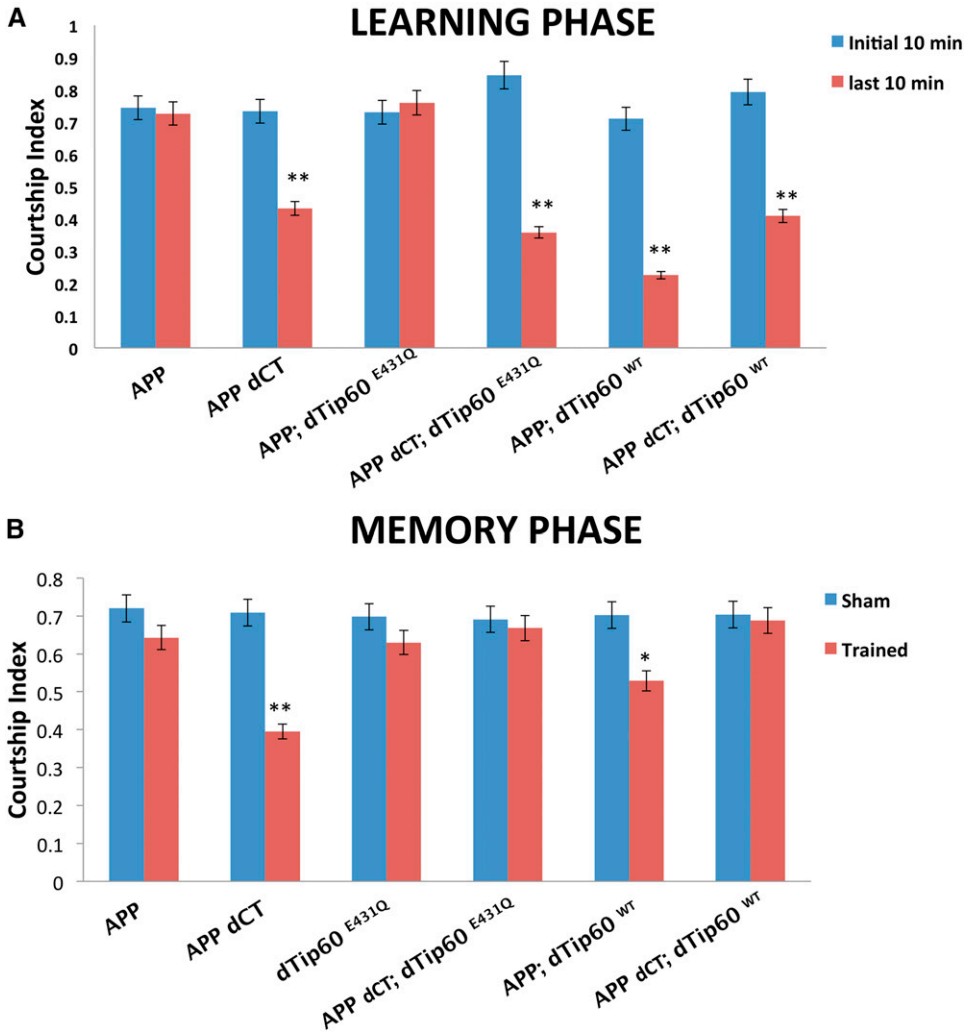

Figure 9 Increased level of Tip60 HAT activity rescues learning and memory deficits under APP-induced neurodegenerative conditions. (A) Learning during the initial 10 min (blue columns) and final 10 min (red columns) of the training phase during the courtship suppression assay. Genotypes are indicated. Flies expressing either hAPP or co-expressing equivalent levels of hAPP with HAT mutant dTip60^{E431Q} exhibit no marked decrease in courtship during final 10 min compared to intitial 10 min, indicative of learning defects. Flies co-expressing hAPP with dTip60^{WT} exhibit marked decrease in courtship index during final 10 min compared to the initial 10 min, indicative of normal learning response. Flies expressing either hAPP dCT or co-expressing and hAPPdCT; dTip60^{E431Q} exhibits marked decrease in courtship index during final 10 min compared to initial 10 min, indicating that learning effects are dependent upon the C-terminal of hAPP. (B) Immediate-recall memory (0–2 min post-training) of trained males compared to untrained (sham) males of the same genotype. Both hAPP and hAPP;dTip60^{E431Q} flies show no significant difference between trained and sham males, indicative of no immediate-recall memory, while hAPP; dTip60^{WT} show significant difference, indicative of memory rescue. hAPP dCT with dTip60^{E431Q} and dTip60^{WT} flies shows no significant difference between trained and sham males, indicative of no immediate recall of training. Error bars represent 95% confidence interval. A single asterisk indicates $P < 0.05$ and a double asterisk indicates $P < 0.001$ compared with sham males. $n = 20$ for trained and untrained males in each genotype.

reported that increasing *in vivo* Tip60 HAT levels in the nervous system of flies under APP-induced neurodegenerative conditions rescues Tip60-mediated, cognition-linked processes impaired in AD that include apoptotic neurodegeneration (Pirooznia *et al.* 2012b), axonal outgrowth (Pirooznia *et al.* 2012a; Pirooznia and Elefant 2013b) and transport (Johnson *et al.* 2013) and restores associated disrupted complex functional abilities that include sleep cycles (Pirooznia *et al.* 2012a; Pirooznia and Elefant 2013b) and locomotor function (Johnson *et al.* 2013). Gene expression analysis revealed that these flies exhibit repression of cassettes of pro-apoptotic genes and induction of pro-survival genes (Pirooznia and Elefant 2012, 2013a; Pirooznia *et al.* 2012b). Together, our results point to an all-encompassing neuroprotective role for Tip60 in early AD progression and support a model by which Tip60 epigenetic reprograms select gene sets that redirect neuronal cell fate from cell death toward cell survival and function (Pirooznia and Elefant 2013a). Tip60 might exert such gene reprogramming either by itself or by complexing with other peptides such as AICD for its recruitment to select genes via promoter-bound TFs such as those that we identified in our ChIP-Seq analysis. Our findings that Tip60 exerts neuroprotective effects under neurodegenerative conditions via epigenetic gene reprogramming are not unprecedented. Indeed, gene transfer of CBP was shown to ameliorate learning and memory deficits in a mouse AD model by increasing brain-derived neurotrophic factor (Caccamo *et al.* 2010), and p300, but not HDAC inhibitors, were found to enhance axonal regeneration by inducing axonal outgrowth genes (Gaub *et al.* 2011). In light of these findings, it is important consider that modulation of specific HAT levels and/or activity may alter the expression of many genes or "cassettes" of specific genes that act together to produce a neuroprotective effect, as indicated by our ChIP-Seq analysis for Tip60 (Pirooznia and Elefant 2012, 2013a). Therefore, it will be critical to determine the identity of

specific cognition-linked gene target sets regulated by Tip60 to further dissect their neuroprotective nature for more effective design of HAT-based therapeutic strategies.

Acknowledgments

We thank Dr. Amita Sehgal for generously contributing a variety of mushroom body GAL4 drivers. This work was supported by National Institutes of Health grant R01HD057939 (to F.E.).

Literature Cited

Akalai, D. B., C. F. Wilson, L. Zong, N. K. Tanaka, K. Ito *et al.*, 2006 Roles for Drosophila mushroom body neurons in olfactory learning and memory. Learn. Mem. 13: 659–668.

Al-Saigh, R., A. Elefanti, A. Velegraki, L. Zerva, and J. Meletiadis, 2012 In vitro pharmacokinetic/pharmacodynamic modeling of voriconazole activity against Aspergillus species in a new in vitro dynamic model. Antimicrob. Agents Chemother. 56: 5321–5327.

Aso, Y., K. Grubel, S. Busch, A. B. Friedrich, I. Siwanowicz *et al.*, 2009 The mushroom body of adult Drosophila characterized by GAL4 drivers. J. Neurogenet. 23: 156–172.

Awasaki, T., M. Saito, M. Sone, E. Suzuki, R. Sakai *et al.*, 2000 The Drosophila trio plays an essential role in patterning of axons by regulating their directional extension. Neuron 26: 119–131.

Baas, P. W., and L. Luo, 2001 Signaling at the growth cone: the scientific progeny of Cajal meet in Madrid. Neuron 32: 981–984.

Baek, S. H., K. A. Ohgi, D. W. Rose, E. H. Koo, C. K. Glass *et al.*, 2002 Exchange of N-CoR corepressor and Tip60 coactivator complexes links gene expression by NF-kappaB and beta-amyloid precursor protein. Cell 110: 55–67.

Barth, M., and M. Heisenberg, 1997 Vision affects mushroom bodies and central complex in Drosophila melanogaster. Learn. Mem. 4: 219–229.

Bates, K. E., C. S. Sung, and S. Robinow, 2010 The unfulfilled gene is required for the development of mushroom body neuropil in Drosophila. Neural Dev. 5: 4.

Borrelli, E., E. J. Nestler, C. D. Allis, and P. Sassone-Corsi, 2008 Decoding the epigenetic language of neuronal plasticity. Neuron 60: 961–974.

Bousiges, O., A. P. Vasconcelos, R. Neidi, B. Cosquer, K. Herbeux *et al.*, 2010 Spatial memory consolidation is associated with induction of several lysine-acetyltransferase (histone acetylatransferase) expression levels and H2B/H4 acetylation-dependent transcriptional events in the rat hippocampus. Neuropsychopharmacology 35: 2521–2537.

Bousiges, O., R. Neidl, M. Majchrzak, M. A. Muller, A. Bergelivien *et al.*, 2013 Detection of histone acetylation levels in the dorsal hippocampus reveals early tagging on specific residues of H2B and H4 histones in response to learning. PLoS ONE 8: e57816.

Broughton, S. J., T. Tully, and R. J. Greenspan, 2003 Conditioning deficits of CaM-kinase transgenic Drosophila melanogaster in a new excitatory courtship assay. J. Neurogenet. 17: 91–102.

Busto, G. U., I. Cervantes-sandoval, and R. L. Davis, 2010 Olfactory learning in Drosophila. Physiology (Bethesda) 26: 338–346.

Caccamo, A., M. A. Maldonado, A. F. Bokov, S. Majumder, and S. Oddo, 2010 CBP gene transfer increases BDNF levels and ameliorates learning and memory deficits in a mouse model of Alzheimer's disease. Proc. Natl. Acad. Sci. USA 107: 22687–22692.

Cao, X., and T. C. Sudhof, 2001 A transcriptionally [correction of transcriptively] active complex of APP with Fe65 and histone acetyltransferase Tip60. Science 293: 115–120.

Cao, X., and T. C. Sudhof, 2004 Dissection of amyloid-beta precursor protein-dependent transcriptional transactivation. J. Biol. Chem. 279: 24601–24611.

Carulli, D., S. Foscarin, and F. Rossi, 2011 Activity-dependent plasticity and gene expression modifications in the adult CNS. Front. Mol. Neurosci. 4: 1–11.

Chawla, S., P. Vanhoutte, F. J. Arnold, C. L. Huang, and H. Bading, 2003 Neuronal activity-dependant nucleocytoplasmic shuttling of HDAC4 and HDAC5. J. Neurochem. 85: 151–159.

Conde, C., and A. Caceres, 2009 Microtubule assembly, organization and dynamics in axons and dendrites. Nat. Rev. Neurosci. 10: 319–332.

Creppe, C., L. Malinouskaya, M. L. Volvert, M. Gillard, P. Close *et al.*, 2009 Elongator controls the migration and differentiation of cortical neurons through acetylation of alpha-tubulin. Cell 136: 551–564.

Crittenden, J. R., E. M. Skoulakis, K. A. Han, D. Kalderon, and R. L. Davis, 1998 Tripartite mushroom body architecture revealed by antigenic markers. Learn. Mem. 5: 38–51.

Dent, E. W., and F. B. Gertler, 2003 Cytoskeletal dynamics and transport in growth cone motility and axon guidance. Neuron 40: 209–227.

Dubnau, J., and T. Tully, 2001 Functional anatomy: from molecule to memory. Curr. Biol. 11: R240–R243.

Ebert, D. H., and M. E. Greenberg, 2013 Activity-dependent neuronal signalling and autism spectrum disorder. Nature 493: 327–337.

Farris, S. M., 2013 Evolution of complex higher brain centers and behaviors: behavioral correlates of mushroom body elaboration in insects. Brain Behav. Evol. 82: 9–18.

Feng, J., S. Fouse, and G. Fan, 2007 Epigenetic regulation of neural gene expression and neuronal function. Pediatr. Res. 61: 58R–63R.

Fiala, A., 2007 Olfaction and olfactory learning in Drosophila: recent progress. Curr. Opin. Neurobiol. 17: 720–726.

Fischer, A., 2014 Targeting histone-modifications in Alzheimer's disease: What is the evidence that this is a promising therapeutic avenue? Neuropharmacology 80: 95–102.

Fushima, K., and H. Tsujimura, 2007 Precise control of fasciclin II expression is required for adult mushroom body development in Drosophila. Dev. Growth Differ. 49: 215–227.

Gaub, P., Y. Joshi, A. Wuttke, U. Naumann, S. Schnichels *et al.*, 2011 The histone acetyltransferase p300 promotes intrinsic axonal regeneration. Brain 134: 2134–2148.

Govindarajan, M., P. Rao, S. Burkhardt, F. Sananbenesi, O. Schluter *et al.*, 2013 Reducing HDAC6 ameliorates cognitive deficits in a mouse model for Alzheimer's disease. EMBO Mol. Med. 5: 52–63.

Graff, J., and I. M. Mansuy, 2008 Epigenetic codes in cognition and behaviour. Behav. Brain Res. 192: 70–87.

Graff, J., D. Rei, J. S. Guan, W. Y. Wang, J. Seo *et al.*, 2012a An epigenetic blockade of cognitive functions in the neurodegenerating brain. Nature 483: 222–226.

Graff, J., B. T. Woldemichael, D. Berchtold, G. Dewarrat, and I. M. Mansuy, 2012b Dynamic histone marks in the hippocampus and cortex facilitate memory consolidation. Nat. Commun. 3: 991.

Greenspan, R. J., 1995 Flies, genes, learning, and memory. Neuron 15: 747–750.

Guan, Z., L. K. Buhl, W. G. Quinn, and J. T. Littleton, 2011 Altered gene regulation and synaptic morphology in Drosophila learning and memory mutants. Learn. Mem. 18: 191–206.

Gunawardena, S., and L. S. Goldstein, 2001 Disruption of axonal transport and neuronal viability by amyloid precursor protein mutations in Drosophila. Neuron 32: 389–401.
Guven-Ozkan, T., and R. L. Davis, 2014 Functional neuroanatomy of Drosophila olfactory memory formation. Learn. Mem. 21: 19.
Heisenberg, M., 2003 Mushroom body memoir: from maps to models. Nat. Rev. Neurosci. 4: 266–275.
Heisenberg, M., M. Heusipp, and C. Wanke, 1995 Structural plasticity in the Drosophila brain. J. Neurosci. 15: 1951–1960.
Hu, A., W. Zhang, and Z. Wang, 2010 Functional feedback from mushroom bodies to antennal lobes in the Drosophila olfactory pathway. Proc. Natl. Acad. Sci. USA 107: 10262–10267.
Johnson, A. A., J. Sarthi, S. K. Pirooznia, W. Reube, and F. Elefant, 2013 Increasing Tip60 HAT levels rescues axonal transport defects and associated behavioral phenotypes in a Drosophila Alzheimer's disease model. J. Neurosci. 33: 7535–7547.
Kahsai, L., and T. Zars, 2011 Learning and memory in Drosophila: behaviour, genetics and neural systems. Int. Rev. Neurobiol. 99: 139–167.
Kazantsev, A. G., and L. M. Thompson, 2008 Therapeutic application of histone deacetylase inhibitors for central nervous system disorders. Nat. Rev. Drug Discov. 7: 854–868.
Keene, A. C., and S. Waddell, 2007 Drosophila olfactory memory: single genes to complex neural circuits. Nat. Rev. Neurosci. 8: 341–354.
Korzus, E., M. G. Rosenfeld, and M. Mayford, 2004 CBP histone acetyltransferase activity is a critical component of memory consolidation. Neuron 42: 961–972.
Lee, T., A. Lee, and L. Luo, 1999 Development of the Drosophila mushroom bodies: sequential generation of three distinct types of neurons from a neuroblast. Development 126: 4065–4076.
Legube, G., and D. Trouche, 2003 Regulating histone acetyltransferases and deacetylases. EMBO Rep. 4: 944–947.
Levenson, J. M., and J. D. Sweatt, 2005 Epigenetic mechanisms in memory formation. Nat. Rev. Neurosci. 6: 108–118.
Levenson, J. M., K. J. O'Riordan, K. D. Brown, M. A. Trinh, D. L. Molfese *et al.*, 2004 Regulation of histone acetylation during memory formation in the hippocampus. J. Biol. Chem. 279: 40545–40559.
Lorbeck, M., K. Pirooznia, J. Sarthi, X. Zhu, and F. Elefant, 2011 Microarray analysis uncovers a role for Tip60 in nervous system function and general metabolism. PLoS ONE 6: e18412.
Luo, L., and D. D. O'Leary, 2005 Axon retraction and degeneration in development and disease. Annu. Rev. Neurosci. 28: 127–156.
Margulies, C., T. Tully, and J. Dubnau, 2005 Deconstructing memory in Drosophila. Curr. Biol. 15: R700–R713.
McBride, S. M., G. Giuliani, C. Choi, P. Krause, D. Correale *et al.*, 1999 Mushroom body ablation impairs short-term memory and long-term memory of courtship conditioning in Drosophila melanogaster. Neuron 24: 967–977.
McBride, S. M., C. H. Choi, Y. Wang, D. Liebelt, E. Braunstein *et al.*, 2005 Pharmacological rescue of synaptic plasticity, courtship behavior, and mushroom body defects in a Drosophila model of fragile X syndrome. Neuron 45: 753–764.
Meaney, M. J., and A. C. Ferguson-Smith, 2010 Epigenetic regulation of the neural transcriptome: the meaning of the marks. Nat. Neurosci. 13: 1313–1318.
Mehren, J. E., A. Ejima, and L. C. Griffith, 2004 Unconventional sex: fresh approaches to courtship learning. Curr. Opin. Neurobiol. 14: 745–750.
Melicharek, D. J., L. C. Ramirez, S. Singh, R. Thompson, and D. R. Marenda, 2010 Kismet/CHD7 regulates axon morphology, memory and locomotion in a Drosophila model of CHARGE syndrome. Hum. Mol. Genet. 19: 4253–4264.
Merdes, G., P. Soba, A. Loewer, M. V. Bilic, K. Beyreuther *et al.*, 2004 Interference of human and Drosophila APP and APP-like proteins with PNS development in Drosophila. EMBO J. 23: 4082–4095.
Morris, R. G., 2003 Long-term potentiation and memory. Philos. Trans. R. Soc. Lond. B Biol. Sci. 358: 643–647.
Muller, T., C. G. Concannon, M. W. Ward, C. M. Walsh, A. L. Tirniceriu *et al.*, 2007 Modulation of gene expression and cytoskeletal dynamics by the amyloid precursor protein intracellular domain (AICD). Mol. Biol. Cell 18: 201–210.
Muller, T., H. E. Meyer, R. Egensperger, and K. Marcus, 2008 The amyloid precursor protein intracellular domain (AICD) as modulator of gene expression, apoptosis, and cytoskeletal dynamics-relevance for Alzheimer's disease. Prog. Neurobiol. 85: 393–406.
Nelson, E. D., and L. M. Monteggia, 2011 Epigenetics in the mature mammalian brain: effects on behavior and synaptic transmission. Neurobiol. Learn. Mem. 96: 53–60.
Peixoto, L., and T. Abel, 2013 The role of histone acetylation in memory formation and cognitive impairments. Neuropsychopharmacology 38: 62–76.
Pirooznia, K., and F. Elefant, 2012 Modulating epigenetic HAT activity: A promising therapuetic option for neurological disease? J. Mol. Cloning Genet. Recomb. 1: 1–3.
Pirooznia, S. K., K. Chiu, M. T. Chan, J. E. Zimmerman, and F. Elefant, 2012a Epigenetic regulation of axonal growth of *Drosophila* pacemaker cells by histone acetyltransferase tip60 controls sleep. Genetics 192: 1327–1345.
Pirooznia, S. K., J. Sarthi, A. A. Johnson, M. S. Toth, K. Chiu *et al.*, 2012b Tip60 HAT activity mediates APP induced lethality and apoptotic cell death in the CNS of a Drosophila Alzheimer's disease model. PLoS ONE 7: e41776.
Pirooznia, K., and F. Elefant, 2013a Targeting specific HATs for neurodegenerative disease treatment: translating basic biology to therapeutic possibilities. Front. Mol. Neurosci. 7: 1–18.
Pirooznia, S. K., and F. Elefant, 2013b A HAT for sleep?: epigenetic regulation of sleep by Tip60 in Drosophila. Fly (Austin) 7: 99–104.
Riccio, A., 2010 Dynamic epigenetic regulation in neurons: enzymes, stimuli and signaling pathways. Nat. Neurosci. 13: 1330–1337.
Ryan, K. A., and S. W. Pimplikar, 2005 Activation of GSK-3 and phosphorylation of CRMP2 in transgenic mice expressing APP intracellular domain. J. Cell Biol. 171: 327–335.
Rybak, J., and R. Menzel, 1993 Anatomy of the mushroom bodies in the honey bee brain: the neuronal connections of the alpha-lobe. J. Comp. Neurol. 334: 444–465.
Sarthi, J., and F. Elefant, 2011 dTip60 HAT activity controls synaptic bouton expansion at the Drosophila neuromuscular junction. PLoS ONE 6: e26202.
Scott, E. K., T. Lee, and L. Luo, 2001 enok encodes a Drosophila putative histone acetyltransferase required for mushroom body neuroblast proliferation. Curr. Biol. 11: 99–104.
Siegel, R. W., and J. C. Hall, 1979 Conditioned responses in courtship behavior of normal and mutant Drosophila. Proc. Natl. Acad. Sci. USA 76: 3430–3434.
Siwicki, K. K., and L. Ladewski, 2003 Associative learning and memory in Drosophila: beyond olfactory conditioning. Behav. Processes 64: 225–238.
Siwicki, K. K., P. Riccio, L. Ladewski, F. Marcillac, L. Dartevelle *et al.*, 2005 The role of cuticular pheromones in courtship conditioning of Drosophila males. Learn. Mem. 12: 636–645.
Slomnicki, L. P., and W. Lesniak, 2008 A putative role of the Amyloid Precursor Protein Intracellular Domain (AICD) in transcription. Acta Neurobiol. Exp. (Warsz.) 68: 219–228.
Sweatt, J. D., 2009 Experience-dependent epigenetic modifications in the central nervous system. Biol. Psychiatry 65: 191–197.
Tabas-Madrid, D., R. Nogales-Cadenas, and A. Pascual-Montano, 2012 GeneCodis3: a non-redundant and modular enrichment

analysis tool for functional genomics. Nucleic Acids Res. 40(Web server issue): W478–W483.
Technau, G. M., 1984 Fiber number in the mushroom bodies of adult Drosophila melanogaster depends on age, sex and experience. J. Neurogenet. 1: 113–126.
von Rotz, R. C., B. M. Kohli, J. Bosset, M. Meier, T. Suzuki *et al.*, 2004 The APP intracellular domain forms nuclear multiprotein complexes and regulates the transcription of its own precursor. J. Cell Sci. 117: 4435–4448.
Watts, R. J., E. D. Hoopfer, and L. Luo, 2003 Axon pruning during Drosophila metamorphosis: evidence for local degeneration and requirement of the ubiquitin-proteasome system. Neuron 38: 871–885.
Watts, R. J., O. Schuldiner, J. Perrino, C. Larsen, and L. Luo, 2004 Glia engulf degenerating axons during developmental axon pruning. Curr. Biol. 14: 678–684.
West, A. E., and M. E. Greenberg, 2011 Neuronal activity-regulated gene transcription in synapse development and cognitive function. Cold Spring Harb. Perspect. Biol. 1: 1–21.
Zhu, X., N. Singh, C. Donnelly, P. Boimel, and F. Elefant, 2007 The cloning and characterization of the histone acetyltransferase human homolog Dmel/TIP60 in *Drosophila melanogaster*: Dmel/TIP60 is essential for multicellular development. Genetics 175: 1229–1240.

Communicating editor: H. J. Bellen

GENETICS

Supporting Information
http://www.genetics.org/lookup/suppl/doi:10.1534/genetics.114.171660/-/DC1

Epigenetic Control of Learning and Memory in *Drosophila* by Tip60 HAT Action

Songjun Xu, Rona Wilf, Trisha Menon, Priyalakshmi Panikker, Jessica Sarthi, and Felice Elefant

DOI: 10.1534/genetics.114.171660

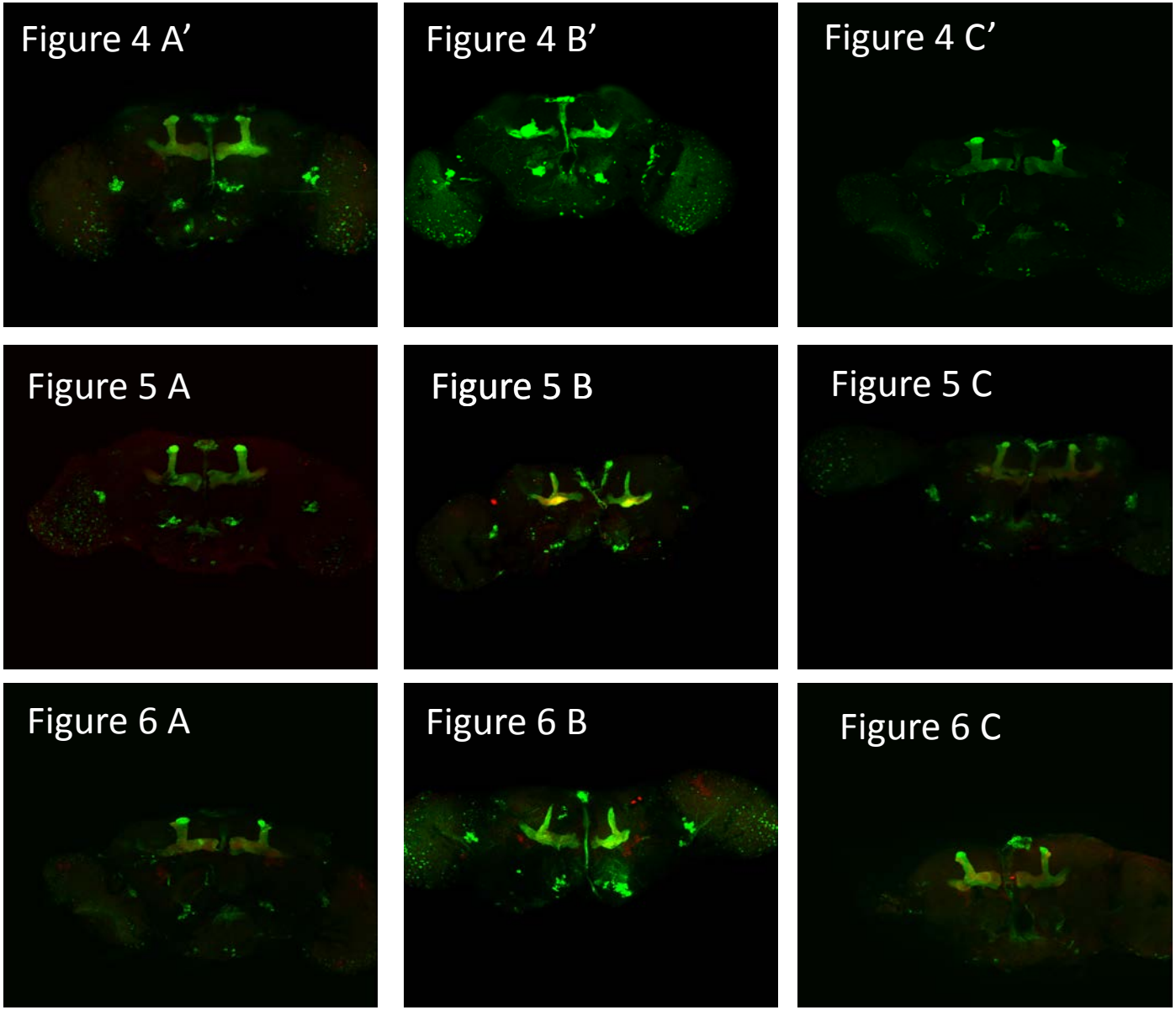

Figure S1 Representative unprocessed confocal images for Figures 4A’-C’; Figures 5A-C and Figures 6A-C. Confocal microscopy was performed using Olympus Microscope with fluoview acquisition software (Olympus, Center Valley, PA). Images were displayed as projections of 1uM serial Z- sections. Consecutive subsets of the Z-stacks were utilized for the final projections.

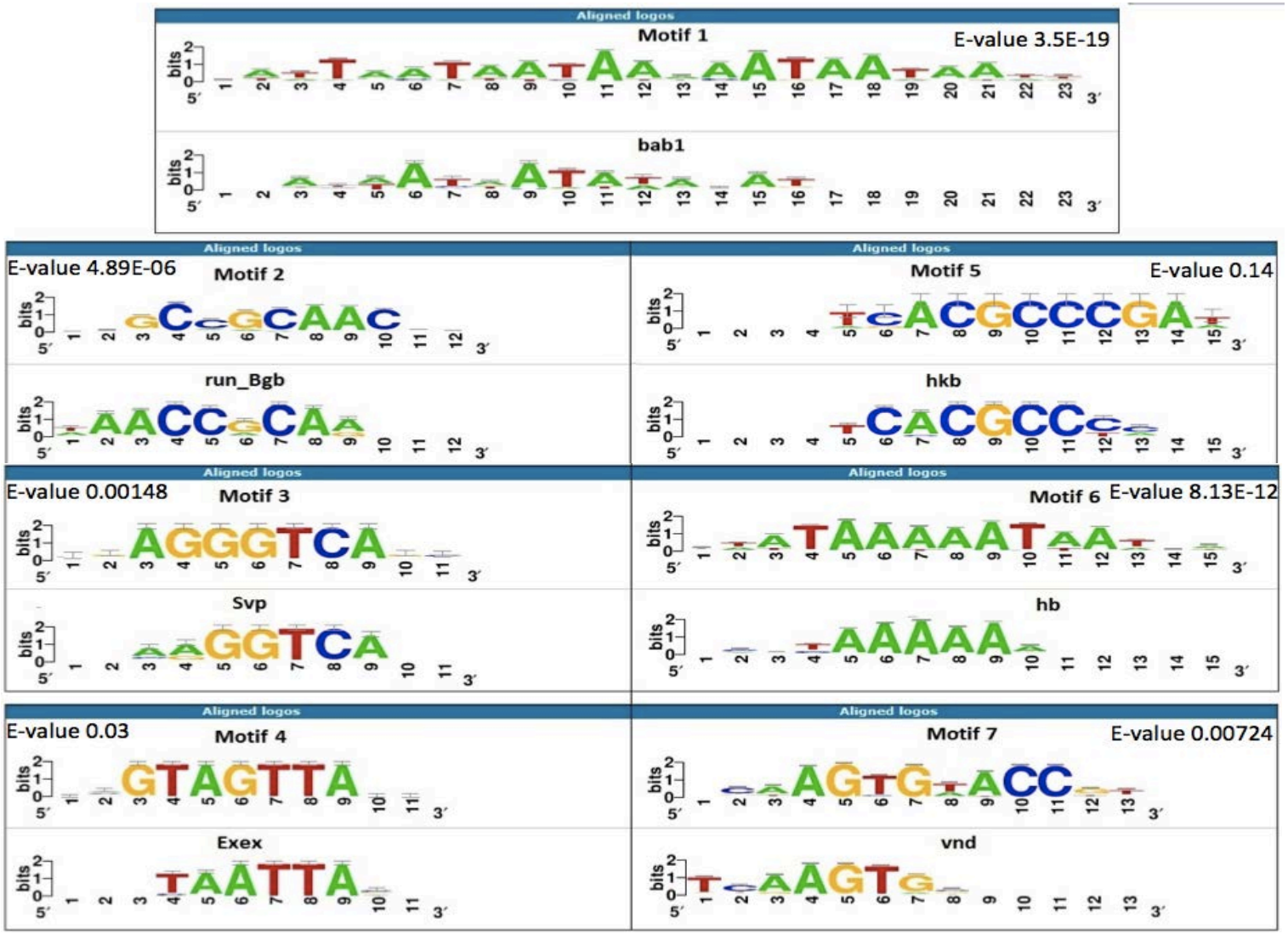

Figure S2 Transcription factor (TF) motifs enriched in Tip60 neuronal gene promoters. TF motifs were identified using the MEME-Chip platform. . Significance values for each discovered motif are represented as E-value (false discovery rate for each pattern search), and matching TF is shown below each match. TFs are bab1 (bric a brac 1) that functions in dendrite arborization, Run-Bgb (big brother), a *Drosophila* CNS TF, Svp (seven up) that functions in CNS development, Exex (extra-extra) that functions in neuroblast development, Hkb (huckebein) that functions in CNS development, Hb (hunchback) that functions in neuroblast fate repression and Vnd (ventral nervous system defective) that functions in brain development.

Table S1 Tip60 gene targets

Gene Symbol	FlyBase ID	Gene Symbol	FlyBase ID	Gene Symbol	FlyBase ID
2mit	FBgn0260793	CG10910	FBgn0034289	CG17514	FBgn0039959
4EHP	FBgn0053100	CG10947	FBgn0032857	CG17839	FBgn0036454
5.8SrRNA:CR40454	FBgn0250731	CG11360	FBgn0039920	CG2121	FBgn0033289
Ac78C	FBgn0024150	CG11873	FBgn0039633	CG30069	FBgn0050069
AGO3	FBgn0250816	CG12061	FBgn0040031	CG30116	FBgn0028496
alpha4GT2	FBgn0039378	CG12502	FBgn0035171	CG30389	FBgn0050389
alpha-Man-I	FBgn0259170	CG12535	FBgn0029657	CG30438	FBgn0050438
Appl	FBgn0000108	CG12541	FBgn0029930	CG31038	FBgn0051038
atms	FBgn0010750	CG12885	FBgn0039523	CG31221	FBgn0051221
bab1	FBgn0004870	CG13300	FBgn0035699	CG31324	FBgn0051324
bab2	FBgn0025525	CG13541	FBgn0034841	CG31619	FBgn0051619
bbg	FBgn0087007	CG13954	FBgn0033405	CG31702	FBgn0051702
beat-IV	FBgn0039089	CG14190	FBgn0030979	CG32373	FBgn0052373
beat-Vb	FBgn0038092	CG14431	FBgn0029922	CG32406	FBgn0052406
bol	FBgn0011206	CG14459	FBgn0037171	CG32486	FBgn0052486
bs	FBgn0004101	CG14636	FBgn0037217	CG32699	FBgn0052699
bxd	FBgn0020556	CG15465	FBgn0029746	CG32700	FBgn0052700
Cap-G	FBgn0259876	CG15831	FBgn0040034	CG32816	FBgn0052816
Ccn	F8gn0052183	CG16781	FBgn0029661	CG32850	FBgn0052850
Cda4	FBgn0052499	CG17018	FBgn0039972	CG32944	FBgn0052944
CR40571	FBgn0085746	CG5036	FBgn0028743	ken	FBgn0011236
CR40572	FBgn0085747	CG6051	FBgn0039492	kirre	FBgn0028369
CR40573	FBgn0085748	CG7369	FBgn0037188	kl-2	FBgn0001313
CR40574	FBgn0085749	CG7564	FBgn0036734	kl-3	FBgn0001314
CR40581	FBgn0085750	CG8861	FBgn0037676	kl-5	FBgn0001315
CR40582	FBgn0085751	CG9766	FBgn0037229	laccase2	FBgn0259247
CR40594	FBgn0085752	CHKov1	FBgn0045761	Lar	FBgn0000464
CR40597	FBgn0085754	chn	FBgn0015371	Lasp	FBgn0063485
CR40611	FBgn0085755	Con	FBgn0005775	lilli	FBgn0041111
CR40613	FBgn0085756	CR32010	FBgn0052010	Liprin-gamma	FBgn0034720
CR40621	FBgn0085757	CR33496	FBgn0053496	LpR2	FBgn0051092
CR40629	FBgn0085505	CR40461	FBgn0058461	luna	FBgn0040765
CR40640	FBgn0085759	CR40502	FBgn0085737	MESR3	FBgn0032694
CR40642	FBgn0085761	CR40503	FBgn0085738	MFS17	FBgn0058263
CR40668	FBgn0085764	CR40508	FBgn0085740	MRP	FBgn0032456
CR40677	FBgn0085765	CR40528	FBgn0085741	mtd	FBgn0013576
CR40679	FBgn0085766	CR40546	FBgn0085742	Muc26B	FBgn0040950
CR40712	FBgn0085768	CR40560	FBgn0085743	Muc30E	FBgn0053300
CR40728	FBgn0085769	CR40561	FBgn0085744	Muc68Ca	FBgn0036181
CR40734	FBgn0085770	CR40565	FBgn0085745	Muc68E	FBgn0053265
su(w[a])	FBgn0003638	SMSr	FBgn0052380	Ppr-Y	FBgn0046697
sxc	FBgn0261403	Snap25	FBgn0011288	pros	FBgn0004595
Syn1	FBgn0037130	Soxl00B	FBgn0024288	Prosap	FBgn0040752
Syt1	FBgn0004242	SPoCk	FBgn0052451	Ptp99A	FBgn0004369
tai	FBgn0041092	spok	FBgn0086917	px	FBgn0003175
Tequila	FBgn0023479	Ste:CG33240	FBgn0053240	raw	FBgn0003209
Tg	FBgn0031975	Ste:CG33241	FBgn0053241	Rbp6	FBgn0260943
timeout	FBgn0038118	Ste:CG33242	FBgn0053242	rl	FBgn0003256
TM4SF	FBgn0020372	SteXh:CG42398	FBgn0259817	roX1	FBgn0019661
toc	FBgn0015600	stnA	FBgn0016976	rut	FBgn0003301
tok	FBgn0004885	Su(Ste):CR42405	FBgn0259836	RYa-R	FBgn0004842
Trim9	FBgn0051721	Su(Ste):CR42407	FBgn0259838	sca	FBgn0003326
twin	FBgn0011725	Su(Ste):CR42418	FBgn0259849	Sdic2	FBgn0053497
Su(Ste):CR42440	FBgn0259871	Sgs1	FBgn0003372	pk	FBgn0003090

Gene Symbol	FlyBase ID	Gene Symbol	FlyBase ID	Gene Symbol	FlyBase ID
CG33158	FBgn0053158	CG40378	FBgn0058378	CR40741	FBgn0085771
CG33170	FBgn0053170	CG40467	FBgn0069977	CR40743	FBgn0085772
CG33267	FBgn0053267	CG40470	FBgn0058470	CR40766	FBgn0085773
CG33988	FBgn0053988	CG40813	FBgn0085521	CR40779	FBgn0085774
CG34031	FBgn0054031	CG40968	FBgn0085546	CR40959	FBgn0085777
CG34104	FBgn0083940	CG41343	FBgn0085625	CR40963	FBgn0085779
CG34106	FBgn0083942	CG41378	FBgn0085638	CR40976	FBgn0085780
CG34347	FBgn0085376	CG41520	FBgn0087011	CR41535	FBgn0085795
CG34353	FBgn0085382	CG41527	FBgn0085670	CR41539	FBgn0085796
CG34355	FBgn0085384	CG41562	FBgn0085693	CR41540	FBgn0085797
CG34356	FBgn0085385	CG42238	FBgn0250867	CR41544	FBgn0085799
CG34376	FBgn0085405	CG42249	FBgn0259101	CR41548	FBgn0085802
CG34417	FBgn0085446	CG42329	FBgn0259229	CR41550	FBgn0085803
CG3544	FBgn0031279	CG42395	FBgn0259741	CR41571	FBgn0085804
CG3726	FBgn0029824	CG42402	FBgn0259821	CR41583	FBgn0085805
CG3777	FBgn0024989	CG42534	FBgn0260487	CR41590	FBgn0085807
CG40006	FBgn0058006	CG42618	FBgn0261281	CR41591	FBgn0085808
CG40155	FBgn0058155	CG42637	FBgn0261360	CR41602	FBgn0085813
CG40160	FBgn0058160	CG4587	FBgn0028863	CR41604	FBgn0085814
CG40178	FBgn0058178	CG5004	FBgn0260748	CR41605	FBgn0085815
heph	FBgn0011224	Dop2R	FBgn0053517	CR41606	FBgn0085816
His1:CG31617	FBgn0051617	dpr6	FBgn0040823	CR41607	FBgn0085817
Hisl:CG33801	FBgn0053801	dpr8	FBgn0052600	CR41608	FBgn0085818
Hìs2A:CG31618	FBgn0051618	Drip	FBgn0015872	CR41609	FBgn0085819
His2B:CG33908	FBgn0053908	ec	FBgn0000542	CR41613	FBgn0085822
His3:CG33866	FBgn0053866	ed	FBgn0000547	CR41617	FBgn0085823
His-Psi:CR31616	FBgn0051616	Eip63E	FBgn0005640	CR41618	FBgn0085824
His-Psi:CR31754	FBgn0051754	Eip75B	FBgn0000568	CR41619	FBgn0085825
His-Psi:CR33802	FBgn0053802	fd102C	FBgn0039937	CR41620	FBgn0085826
His-Psi:CR33805	FBgn0053805	fne	FBgn0086675	CR41621	FBgn0085827
hoe1	FBgn0041150	for	FBgn0000721	CR42195	FBgn0085828
InR	FBgn0013984	Fs	FBgn0259878	Cyp309a2	FBgn0041337
Ir40a	FBgn0259683	ftz-f1	FBgn0001078	d4	FBgn0033015
Ir4la	FBgn0040849	Fur1	FBgn0004509	Dbp80	FBgn0024804
Ir93a	FBgn0259215	gammaTry	FBgn0010359	Dgk	FBgn0085390
JlL-1	FBgn0020412	Gas8	FBgn0029667	Dh44-R2	FBgn0033744
jim	FBgn0027339	GEFmeso	FBgn0050115	dnc	FBgn0000479
KCNQ	FBgn0033494	Gprkl	FBgn0260798	dnr1	FBgn0260866
kek2	FBgn0015400	GS	FBgn0030882	dnt	FBgn0024245
kek5	FBgn0031016	Haspin	FBgn0046706	Dop1Rl	FBgn0011582
Muc96D	FBgn0051439	Shawl	FBgn0085395	Pka-C3	FBgn0000489
Nipped-A	FBgn0053554	SK	FBgn0029761	Pka-R1	FBgn0259243
NIg2	FBgn0031866	skd	FBgn0003415	pIexB	FBgn0025740
nmo	FBgn0011817	Su(Ste):CR42443	FBgn0259874	sky	FBgn0032901
nvd	FBgn0259697	Ppl-Y2	FBgn0046698	SKIP	FBgn0051163
OdsH	FBgn0026058	unc-5	FBgn0034013	Su(Ste):CR42435	FBgn0259866
Ory	FBgn0046323	vtd	FBgn0260987	Su(Ste):CR42436	FBgn0259867
Papss	FBgn0020389	X11Lbeta	FBgn0052677	Su(Ste):CR42439	FBgn0259870
Parp	FBgn0010247	plum	FBgn0039431	Su(Ste):CR42442	FBgn0259873
pb	FBgn0051481	Ppl-Y1	FBgn0261399	sIs	FBgn0086906
Pc	FBgn0003042	Ubi-p63E	FBgn0003943	Su(Ste):CR42420	FBgn0259851
PH4alphaEFB	FBgn0039776	uif	FBgn0031879	Su(Ste):CR42425	FBgn0259856
phI	FBgn0003079	Sema-1a	FBgn0011259	pigs	FBgn0029881
-	-	-	-	-	-

Table S2 Tip60 neuronal gene targets

Gene Symbol	FlyBase ID	Gene Symbol	FlyBase ID	Gene Symbol	FlyBase ID
2mit	FBgn0260793	CG33988	FBgn0053988	Elp63E	FBgn0005640
Ac78C	FBgn0024150	CG34104	FBgn0083940	Elp75B	FBgn0000568
alpha-Man-I	FBgn0259170	CG34106	FBgn0083942	fd102C	FBgn0039937
Appl	FBgn0000108	CG34347	FBgn0085376	fne	FBgn0086675
atms	FBgn0010750	CG34353	FBgn0085382	for	FBgn0000721
bab1	FBgn0004870	CG34355	FBgn0085384	Fs	FBgn0259878
bab2	FBgn0025525	CG34356	FBgn0085385	ftz-f1	FBgn0001078
bbg	FBgn0087007	CG34376	FBgn0085405	Fur1	FBgn0004509
beat-IV	FBgn0039089	CG34417	FBgn0085446	Gas8	FBgn0029667
beat-Vb	FBgn0038092	CG3726	FBgn0029824	GEFmeso	FBgn0050115
bol	FBgn0011206	CG40006	FBgn0058006	Gprk1	FBgn0260798
bs	FBgn0004101	CG40155	FBgn0058155	GS	FBgn0030882
Cap-G	FBgn0259876	CG40160	FBgn0058160	Haspin	FBgn0046706
Ccn	FBgn0052183	CG40178	FBgn0058178	heph	FBgn0011224
Cda4	FBgn0052499	CG40378	FBgn0058378	His3:CG33866	FBgn0053866
CG11360	FBgn0039920	CG40467	FBgn0069977	His-Psi:CR31754	FBgn0051754
CG12502	FBgn0035171	CG40470	FBgn0058470	hoe1	FBgn0041150
CG12541	FBgn0029930	CG41520	FBgn0087011	lnR	FBgn0013984
CG12885	FBgn0039523	CG42329	FBgn0259229	Ir41a	FBgn0040849
CG13300	FBgn0035699	CG4587	FBgn0028863	JIL-1	FBgn0020412
CG14431	FBgn0029922	CG5036	FBgn0028743	jim	FBgn0027339
CG14459	FBgn0037171	CG8861	FBgn0037676	KCNQ	FBgn0033494
CG14636	FBgn0037217	CG9766	FBgn0037229	kek2	FBgn0015400
CG15465	FBgn0029746	CHKov1	FBgn0045761	kek5	FBgn0031016
CG15831	FBgn0040034	chn	FBgn0015371	ken	FBgn0011236
CG17514	FBgn0039959	Con	FBgn0005775	kirre	FBgn0028369
CG17839	FBgn0036454	CR32010	FBgn0052010	kl-2	FBgn0001313
CG2121	FBgn0033289	CR41604	FBgn0085814	laccase2	FBgn0259247
CG30069	FBgn0050069	Cyp309a2	FBgn0041337	Lar	FBgn0000464
CG30116	FBgn0028496	d4	FBgn0033015	lilli	FBgn0041111
CG30389	FBgn0050389	Dbp80	FBgn0024804	Liprin-gamma	FBgn0034720
CG31038	FBgn0051038	Dgk	FBgn0085390	luna	FBgn0040765
CG31221	FBgn0051221	Dh44-R2	FBgn0033744	MFS17	FBgn0058263
CG31324	FBgn0051324	dnc	FBgn0000479	mtd	FBgn0013576
CG31619	FBgn0051619	dnr1	FBgn0260866	Muc96D	FBgn0051439
CG32406	FBgn0052406	dnt	FBgn0024245	Nipped-A	FBgn0053554
CG32486	FBgn0052486	Dop1R1	FBgn0011582	Nlg2	FBgn0031866
CG32700	FBgn0052700	Dop2R	FBgn0053517	nmo	FBgn0011817
CG32816	FBgn0052816	dpr6	FBgn0040823	Papss	FBgn0020389
CG32850	FBgn0052850	dpr8	FBgn0052600	Parp	FBgn0010247
CG32944	FBgn0052944	Drip	FBgn0015872	pb	FBgn0051481
CG33158	FBgn0053158	ec	FBgn0000542	Pc	FBgn0003042
CG33170	FBgn0053170	ed	FBgn0000547	PH4alphaEFB	FBgn0039776

Gene Symbol	FlyBase ID	Gene Symbol	FlyBase ID
phl	FBgn0003079	SMSr	FBgn0052380
pigs	FBgn0029881	Snap25	FBgn0011288
pk	FBgn0003090	SPoCk	FBgn0052451
Pka-C3	FBgn0000489	spok	FBgn0086917
Pka-R1	FBgn0259243	Ste:CG33240	FBgn0052340
plexB	FBgn0025740	Ste:CG33241	FBgn0053241
plum	FBgn0039431	Ste:CG33242	FBgn0053242
pros	FBgn0004595	stnA	FBgn0016976
Prosap	FBgn0040752	su(w[a])	FBgn0003638
Ptp99A	FBgn0004369	sxc	FBgn0261403
px	FBgn0003175	Syn1	FBgn0037130
raw	FBgn0003209	Syt1	FBgn0004242
Rbp6	FBgn0260943	tai	FBgn0041092
rl	FBgn0003256	Tequila	FBgn0023479
rut	FBgn0003301	Tg	FBgn0031975
RYa-R	FBgn0004842	TM4SF	FBgn0020372
sca	FBgn0003326	toc	FBgn0015600
Sdic2	FBgn0053497	tok	FBgn0004885
Sema-1a	FBgn0011259	Trim9	FBgn0051721
Shawl	FBgn0085395	Ubi-p63E	FBgn0003943
SK	FBgn0029761	uif	FBgn0031879
skd	FBgn0003415	unc-5	FBgn0034013
SKIP	FBgn0051163	vtd	FBgn0260987
sky	FBgn0032901	x11Lbeta	FBgn0052677
sls	FBgn0086906	-	-